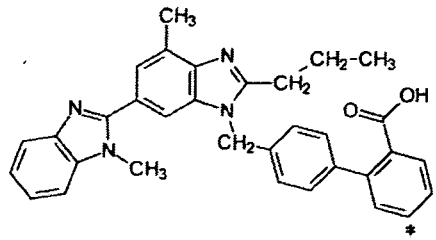

FIG. 1. Chemical structure of [^{3}H]telmisartan. The asterisk denotes the position of the ^{3}H-label.

pressed on the sinusoidal membrane of hepatocytes and are thought to be involved in the transport of a wide variety of compounds including clinically used drugs, such as 3-hydroxy-3-methylglutaryl CoA reductase inhibitors (statins), from blood into hepatocytes (Abe et al., 1999; Hsiang et al., 1999; Kok et al., 2000; Konig et al., 2000a,b; Tamai et al., 2000; Faber et al., 2003; Hirano et al., 2004). In particular, OATP1B1 and OATP1B3 are mainly expressed in human liver (Hagenbuch and Meier, 2003), and the substrate specificity of OATP1B3 commonly overlaps that of OATP1B1, so several compounds can be bisubstrates of both OATP1B1 and OATP1B3, such as estradiol 17β-D-glucuronide ($E_2$17βG), pitavastatin, and rifampicin (Vavricka et al., 2002; Hirano et al., 2004). Hirano et al. (2004) have recently established methods for estimating the contribution of OATP1B1 and OATP1B3 to the hepatic uptake of a number of compounds. They have shown that pitavastatin and $E_2$17βG are taken up in human hepatocytes mainly by OATP1B1. On the other hand, the uptake of fexofenadine, an H_1 receptor antagonist, was mainly mediated by OATP1B3 rather than OATP1B1 (Shimizu et al., 2005). This kind of information is helpful for predicting the effect of changes in expression level and function of certain transporters caused by genetic polymorphisms, pathophysiological conditions, and transporter-mediated drug-drug interactions on the overall hepatic uptake clearance and subsequent pharmacokinetics of drugs. Moreover, if compounds can selectively inhibit OATP1B1- or OATP1B3-mediated transport, we can also easily calculate the contribution of each transporter to the uptake of particular compounds in human hepatocytes by estimating the fraction of their uptake that can be inhibited by transporter-selective inhibitors. However, our preliminary study and a previous report showed that cholecystokinin octapeptide (CCK-8) could also inhibit OATP1B1-mediated transport (Nozawa et al., 2003), indicating that it cannot be used as an OATP1B3-selective inhibitor, although it is selectively transported by OATP1B3 (Ismair et al., 2001). On the other hand, there is little information about selective inhibitors against OATP1B1.

Therefore, the aim of our study is to show the involvement of OATP family transporters in the hepatic uptake process of telmisartan and estimate the contribution of OATP1B1 and OATP1B3 to its uptake in human hepatocytes by a newly developed estimation method using the OATP1B1-selective inhibitor estrone-3-sulfate (E-sul).

Materials and Methods

Chemicals. [^{3}H]Telmisartan (762 GBq/mmol, radiochemical purity >98%), 4′-[(1,4′-dimethyl-2′-propyl[2,6′-bi-1*H*-benzimidazol]-1′-yl)methyl]-[1,1′-biphenyl]-2-carboxylic acid, and unlabeled telmisartan were synthesized by Boehringer Ingelheim Pharma KG (Biberach, Germany) (Ries et al., 1993). [^{3}H]$E_2$17βG, [^{3}H]E-sul, and [^{3}H]taurocholate were purchased from PerkinElmer Life and Analytical Sciences (Boston, MA). [^{3}H]CCK-8 was purchased from Amersham Biosciences UK Ltd. (Little Chalfont, Buckinghamshire, UK). Unlabeled $E_2$17βG, E-sul, taurocholate, CCK-8, and digoxin were purchased from Sigma-Aldrich (St. Louis, MO). Pravastatin and tetraethylammonium (TEA) were obtained from Wako Pure Chemicals (Kyoto, Japan). All the other chemicals and reagents were commercial products of reagent grade.

Cell Culture. OATP1B1-, OATP1B3-, and OATP2B1-expressing or vector-transfected human embryonic kidney (HEK) 293 cells were established previously (Hirano et al., 2004; Shimizu et al., 2005). HEK293 cells were grown in Dulbecco's modified Eagle's medium low glucose (Invitrogen, Carlsbad, CA) supplemented with 10% fetal bovine serum (Invitrogen), 100 U/ml penicillin, 100 μg/ml streptomycin, and 0.25 μg/ml amphotericin B at 37°C with 5% CO_2 and 95% humidity. Cells were then seeded in 12-well plates [coated with 50 mg/l poly(L-lysine) and 50 mg/l poly(L-ornithine); Sigma] at a density of 1.5×10^5 cells/well. For the transport study, the cell culture medium was replaced with culture medium supplemented with 5 mM sodium butyrate for 24 h before transport assay to induce the expression of transporters.

Transport Study Using Transporter Expression Systems. The transport study was carried out as described previously (Hirano et al., 2004). Uptake was initiated by adding Krebs-Henseleit buffer (118 mM NaCl, 23.8 mM $NaHCO_3$, 4.8 mM KCl, 1.0 mM KH_2PO_4, 1.2 mM $MgSO_4$, 12.5 mM HEPES, 5.0 mM glucose, and 1.5 mM $CaCl_2$ adjusted to pH 7.4) containing radiolabeled and unlabeled substrates after cells had been washed twice and preincubated with Krebs-Henseleit buffer at 37°C for 15 min. The uptake was terminated at designated times by adding ice-cold Krebs-Henseleit buffer after removal of the incubation buffer. Then, cells were washed twice with 1 ml of ice-cold Krebs-Henseleit buffer, solubilized in 1 N NaOH, and kept for 1 h at 37°C. Aliquots were transferred to scintillation vials after adding a half volume of 2 N HCl. The radioactivity associated with the cells and incubation buffer was measured in a liquid scintillation counter (TRI-CARB 2500TR, PerkinElmer) after adding 2 ml of scintillation fluid. The remaining 50 μl of cell lysate was used to determine the protein concentration by the method of Lowry with bovine serum albumin as a standard.

Preparation of Rat and Human Hepatocytes. Isolated rat hepatocytes were prepared from Sprague-Dawley rats weighing 200 to 300 g by the collagenase perfusion method described previously (Yamazaki et al., 1993). Isolated hepatocytes (viability >80%) were suspended in Krebs-Henseleit buffer, adjusted to 2.0×10^6 cells/ml, and stored on ice before the uptake experiment. Cryopreserved human hepatocytes (lot. OCF, MYO, and 094) were purchased from In Vitro Technologies, Inc. (Baltimore, MD). The preparation of hepatocytes was performed as described previously (Shitara et al., 2003). The cryopreserved human hepatocytes were resuspended in Krebs-Henseleit buffer to give a final cell density of 1.0×10^6 viable cells/ml for the uptake study. The number of viable cells was determined by trypan blue staining. To measure the uptake in the absence of Na^+, sodium chloride and sodium bicarbonate in Krebs-Henseleit buffer were replaced with choline chloride and choline bicarbonate.

Transport Study Using Hepatocytes. Before the uptake studies, the cell suspensions were prewarmed at 37°C for 3 min. The uptake studies were initiated by adding an equal volume of buffer (120–200 μl) containing labeled and unlabeled substrates to the cell suspension. After incubation at 37°C for 0.5, 2, or 5 min, the reaction was terminated by separating the cells from the substrate solution. For this purpose, an aliquot of 80 μl of incubation mixture was collected and placed in a centrifuge tube (450 μl) containing 50 μl of 2 N NaOH under a layer of 100 μl of oil mixture (density, 1.015, a mixture of silicone oil and mineral oil; Sigma-Aldrich), and subsequently the sample tube was centrifuged for 20 s using a standard centrifuge (17,500*g*, MX-100, TOMY). During this process, hepatocytes passed through the oil layer into the alkaline solution. After an overnight incubation in alkali to dissolve the hepatocytes and the centrifuge tube was frozen in liquid nitrogen, the centrifuge tube was cut, and each compartment was transferred to a scintillation vial. The compartment containing the dissolved cells was neutralized with 50 μl of 2 N HCl. The aliquots were mixed with scintillation mixture, and the radioactivity was measured in a liquid scintillation counter.

Estimation of Protein Unbound Concentration of Telmisartan in the Presence of Human Serum Albumin. The unbound concentration of 1 μM telmisartan in the presence of human serum albumin (HSA) (0, 0.1, 0.3, 1, 3, and 5%) was determined after a 2-h incubation at 37°C by equilibrium dialysis (DIANORM, Dainippon Pharmaceutical Ltd., Osaka, Japan).

Kinetic Analyses. Ligand uptake was expressed as the uptake volume

(microliters per milligram protein), given as the radioactivity associated with the cells (disintegrations per milligram protein) divided by its concentration in the incubation media (disintegrations per microliter). Specific uptake was obtained by subtracting the uptake into vector-transfected cells from the uptake into cDNA-transfected cells. Kinetic parameters were obtained using eq. 1:

$$v = \frac{V_{max} \times S}{K_m + S} \quad (1)$$

where v is the uptake velocity of the substrate (picomoles per minute per milligram protein), S is the substrate concentration in the medium (micromolar), K_m is the Michaelis constant (micromolar), and V_{max} is the maximum uptake rate (picomoles per minute per milligram protein). Fitting was performed by the nonlinear least-squares method using a MULTI program (Yamaoka et al., 1981). The half-inhibitory concentration (IC_{50}) of inhibitors was obtained by examining their inhibitory effects on the uptake of CCK-8, $E_2$17βG, and telmisartan based on eq. 2:

$$CL_{+I} = CL/\left(1 + \frac{I}{IC_{50}}\right) \quad (2)$$

where CL and CL_{+I} represent the uptake clearance in the absence and presence of inhibitor, respectively, and I is the concentration of inhibitor. IC_{50} values were estimated by the nonlinear least-squares method using a MULTI program (Yamaoka et al., 1981). To determine the saturable hepatic uptake clearance in rat and human hepatocytes, we first determined the hepatic uptake clearance [$CL_{(2\ min-0.5\ min)}$] (microliters per minute per 10^6 cells) by calculating the slope of the uptake volume (V_d) (microliters per 10^6 cells) between 0.5 and 2 min (eq. 3). The hepatic uptake clearance was fitted to eq. 1 by means of nonlinear least-squares regression analysis using a MULTI program (Yamaoka et al., 1981). The saturable hepatic uptake clearance (CL_{hep}) was determined by subtracting $CL_{(2\ min-0.5\ min)}$ in the presence of an excess of unlabeled substrate (excess) from that in the absence of unlabeled substrate (tracer) (eq. 4).

$$CL_{(2\ min-0.5\ min)} = \frac{V_{d,2\ min} - V_{d,0.5\ min}}{2 - 0.5} \quad (3)$$

$$CL_{hep} = CL_{(2\ min-0.5\ min),tracer} - CL_{(2\ min-0.5\ min),excess} \quad (4)$$

Estimation of the Maximum Unbound Concentration of Inhibitors at the Liver Inlet. The maximum unbound concentration at the liver inlet ($I_{in,max,u}$) was calculated from the following equation (eq. 5) as described previously (Ito et al., 1998).

$$I_{in,max,u} = \left(C_{max,blood} + \frac{k_a \cdot D \cdot F_a}{Q_h}\right) \times f_{u,blood} \quad (5)$$

where $C_{max,blood}$ and $f_{u,blood}$ are estimated by the reported values of the maximum blood concentration of drug after p.o. administration of the clinical dose (D = 160 mg) and the plasma protein unbound fraction (0.005) and blood-to-plasma concentration ratio (about 1.0) in humans (Stangier et al., 2000a,b). Q_h is the hepatic blood flow rate (96.6 l/h). To avoid the false-negative prediction, k_a is set to a theoretically maximum absorption rate constant (6/h), and F_a is set to one.

Statistical Analysis. The two-tailed Dunnett test was used to assess the significance of differences between three sets of data. Differences were considered to be statistically significant when $P < 0.05$.

Results

Uptake of Telmisartan into Isolated Rat Hepatocytes. Telmisartan was taken up into isolated rat hepatocytes in a time-dependent manner. Whereas saturation of the uptake of telmisartan by an excess of unlabeled telmisartan (40 μM) was not clearly observed in the incubation media with 0 and 0.1% HSA, it could be observed in the presence of 0.3 to 5% HSA (Fig. 2, A–F). Thus, we decided to evaluate the telmisartan uptake with more than 0.3% of HSA in the incubation media to prevent its extensive adsorption to the cells and culture materials. The protein unbound fraction of telmisartan in the incubation media with 0.3, 1, 3, and 5% HSA was 0.056, 0.018, 0.006, and 0.004, respectively. Both the uptake and the unbound fraction of telmisartan were reduced in parallel as the concentration of HSA was increased (Fig. 2G). In the presence of 1% HSA, telmisartan was taken up into isolated rat hepatocytes linearly up to 5 min (Fig. 3A). The concentration dependence of the uptake of telmisartan was studied over concentration range of 0.1 to 40 μM in the presence of 1% HSA. Eadie-Hofstee plot showed one saturable component (Fig. 3B), and the apparent K_m and V_{max} values for telmisartan uptake in the presence of 1% HSA were 21.7 ± 4.4 μM and 371 ± 58 pmol/min/10^6 cells, respectively. Depletion of Na^+ in the incubation media did not affect the uptake of telmisartan (Fig. 4A), and the uptake was inhibited by pravastatin, digoxin, and taurocholate, which are substrates and inhibitors of Oatp isoforms, with IC_{50} values of 58.6 ± 15.5, 45.3 ± 11.7, and 300 ± 99 μM, respectively. However, 1 mM TEA, a typical substrate of organic cation transporter, did not affect the uptake of telmisartan (Fig. 4B).

Uptake of Telmisartan by Transporter-Expressing HEK293 Cells. In the transport study using transporter expression systems, we reduced the HSA concentration from 1% to 0.3% in the incubation media because only a minimal transport activity of $E_2$17βG, which is used as the probe substrate for OATP1B1, was detected in OATP1B1-expressing cells in the presence of 1% HSA because of the significant decrease in its unbound concentration by binding to HSA (vector-transfected control cells, 2.32 ± 0.21 μl/2 min/mg protein; OATP1B1-expressing cells, 3.95 ± 0.21 μl/2 min/mg protein). To identify which transporters are important for the hepatic uptake of telmisartan in humans, the uptake assay was carried out using OATP1B1- and OATP1B3-expressing HEK293 cells in the presence of 0.3% HSA in the incubation media. Under these conditions, significant uptake of $E_2$17βG by OATP1B1- and OATP1B3-expressing HEK293 cells was observed (Fig. 5B). On the other hand, telmisartan was taken up by OATP1B3 but not by OATP1B1 (Fig. 5A). Because the difference in the degree of uptake between vector- and OATP1B3-transfected cells was too small to assess its saturation kinetics in the presence of 0.3% HSA, the concentration dependence of telmisartan uptake was evaluated over the concentration range of 0.05 to 10 μM in the absence of HSA at 5 min. The K_m and V_{max} values of telmisartan transport by OATP1B3 were calculated to be 0.81 ± 0.18 μM and 6.7 ± 0.91 pmol/min/mg protein, respectively (Fig. 6).

Inhibitory Effect of E-sul on OATP1B1- and OATP1B3-Mediated Uptake of Telmisartan in Transporter-Expression Systems. The inhibitory effect of E-sul on OATP1B1- and OATP1B3-mediated uptake of $E_2$17βG, CCK-8, and telmisartan was evaluated using OATP1B1- and OATP1B3-expressing HEK293 cells in the presence of 0.3% HSA. E-sul strongly inhibited OATP1B1-mediated $E_2$17βG uptake with an IC_{50} value of 0.79 ± 0.51 μM, whereas E-sul did not inhibit the OATP1B3-mediated CCK-8 uptake up to 30 μM (IC_{50} = 97.1 ± 37 μM) (Fig. 7A). In addition, the OATP1B3-mediated uptake of telmisartan was not inhibited by 30 μM E-sul (Fig. 7B).

Uptake of Telmisartan into Cryopreserved Human Hepatocytes. The uptake of 1 μM $E_2$17βG and 0.1 μM telmisartan by three different batches of cryopreserved human hepatocytes (lot. OCF, 094, and MYO) in the presence of 0.3% HSA was increased from 0.5 to 2 min [uptake of $E_2$17βG and telmisartan by cryopreserved human hepatocytes (OCF): 6.3 ± 1.0 and 56.7 ± 3.6 μl/min/10^6 cells, respectively], and their uptake was reduced in the presence of an excess of unlabeled $E_2$17βG (200 μM) and telmisartan (40 μM) to 0.6 ± 1.1 and 8.2 ± 4.7 μl/min/10^6 cells, respectively. The uptake of $E_2$17βG into human hepatocytes was inhibited by more than half at 30 μM E-sul, whereas that of telmisartan was not significantly inhibited by 30 μM E-sul (Table 1).

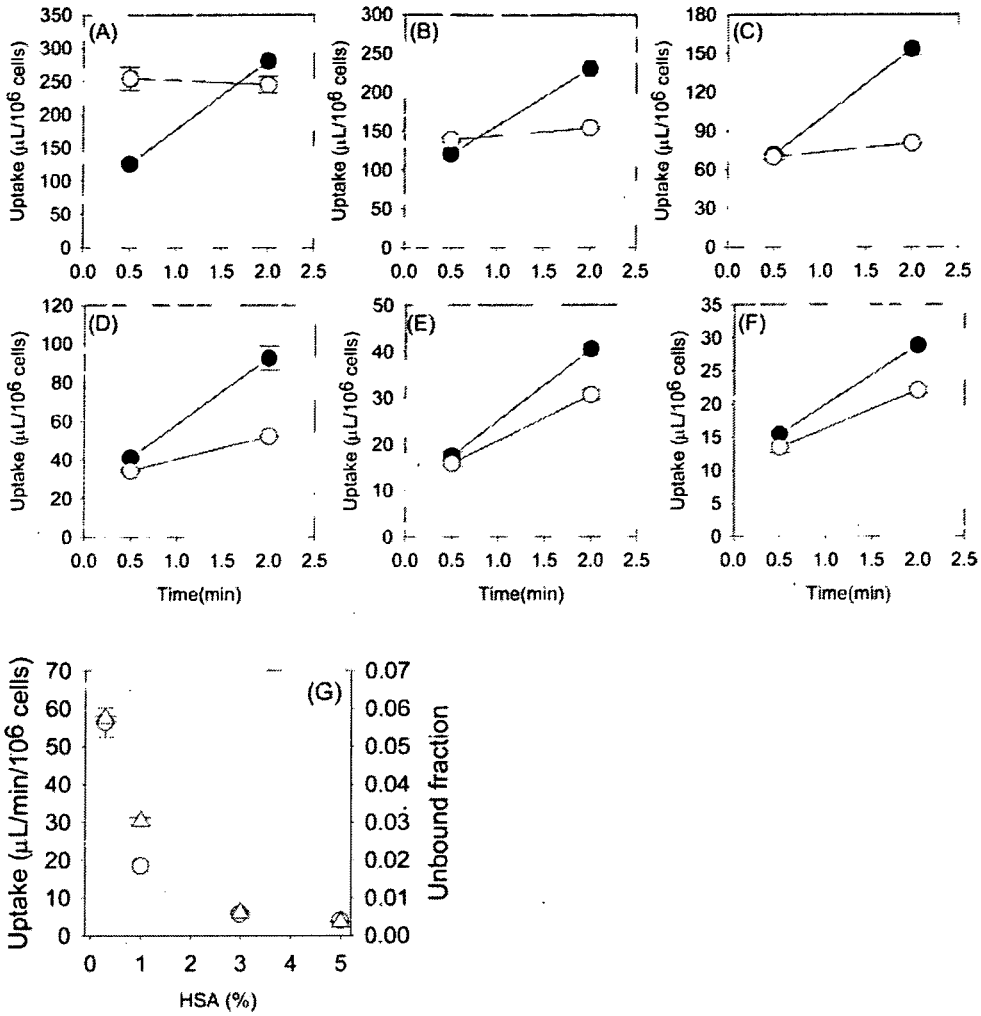

FIG. 2. Effect of various concentrations of HSA on the uptake of telmisartan in isolated rat hepatocytes and the unbound fraction of telmisartan. Uptake of telmisartan was measured by incubating cells with 0.1 μM (closed circle) and 40 μM (open circle) telmisartan, and saturable uptake of telmisartan by isolated rat hepatocytes was determined using eq. 3 and eq. 4. HSA concentrations used were 0 (A), 0.1 (B), 0.3 (C), 1 (D), 3 (E), and 5% (F). G, triangles and circles represent the uptake of telmisartan into isolated rat hepatocytes (μl/min/10^6 cells) and unbound fraction of telmisartan, respectively. Each point represents the mean ± S.E. of three separate determinations.

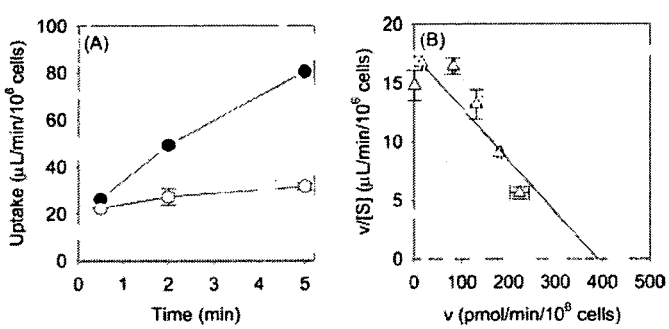

FIG. 3. Time profile (A) and Eadie-Hofstee plot (B) of the uptake of telmisartan by isolated rat hepatocytes in the presence of 1% HSA. A, substrate concentrations used were 0.1 (closed circles) and 40 μM (open circles). B, the uptake of telmisartan in isolated rat hepatocytes was measured at a concentration between 0.1 and 40 μM telmisartan. The initial uptake rate of telmisartan in isolated rat hepatocytes was determined using eq. 3. The solid line represents the fitted curve. Each point represents the mean ± S.E. of three separate determinations.

Discussion

In the present study, we have shown that telmisartan is likely to be taken up into rat and human hepatocytes by OATP family transporters because the uptake was Na^+-independent and inhibited by some OATP substrates/inhibitors. We also have suggested that OATP1B3 predominantly contributes to the hepatic uptake of telmisartan in human hepatocytes.

Because it is difficult to evaluate the transport of telmisartan in the absence of HSA because of the extensive adsorption of lipophilic telmisartan to cells and/or culture materials, we examined the effect of different concentrations of HSA (0.1–5%) in the incubation media on the uptake of telmisartan by isolated rat hepatocytes (Fig. 2, A–F). In 0.3 to 5% HSA, saturable time-dependent uptake of telmisartan was clearly observed. The uptake of telmisartan into isolated rat hepatocytes was almost proportional to the protein unbound concentration of telmisartan in the incubation media, suggesting that the uptake of telmisartan followed the "free" hypothesis, in which only unbound ligand can be recognized by transporters (Fig. 2G).

Taking the balance between the absolute uptake amount and the avoidance of extensive adsorption of telmisartan to cells and/or culture materials by HSA into consideration, we decided to use 1 and 0.3% HSA in the incubation media for the further evaluation of telmisartan uptake by rat and human hepatocytes, respectively.

Initially, we characterized the transport property of telmisartan using isolated rat hepatocytes. Telmisartan was transported into isolated rat hepatocytes in a time- and concentration-dependent manner

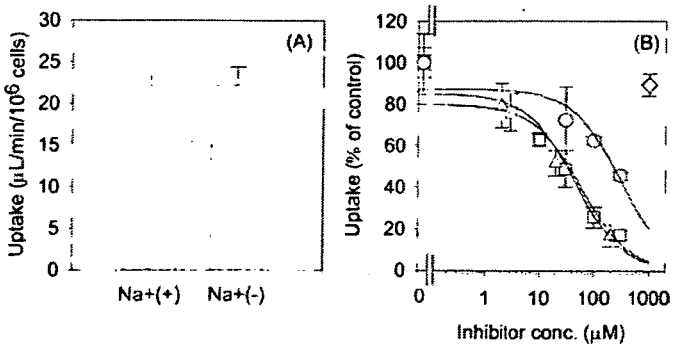

FIG. 4. Effect of Na^+ ion (A) and various compounds (B) on the uptake of telmisartan in isolated rat hepatocytes in the presence of 1% HSA. The substrate concentration used was 0.1 μM. Saturable uptake of telmisartan by isolated rat hepatocytes was determined using eq. 3 and eq. 4. B, data are shown as the percentage of the saturable uptake of telmisartan in the absence of inhibitors. Squares, triangles, circles, and diamonds represent the uptake of telmisartan in the presence of pravastatin, digoxin, taurocholate, and tetraethylammonium, respectively. Solid lines represent the fitted curves obtained by nonlinear regression analysis. Each bar and point represents the mean ± S.E. of three separate determinations.

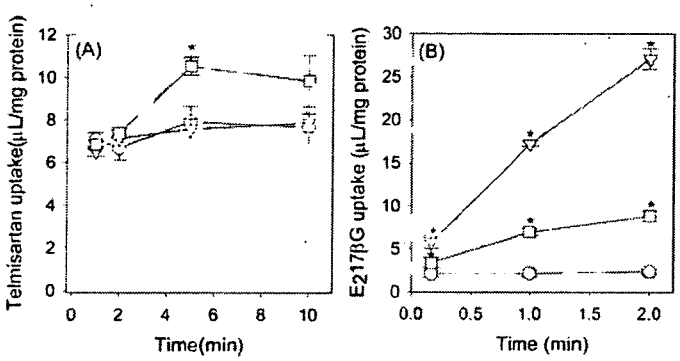

FIG. 5. Time profiles of the uptake of telmisartan (A) and $E_2 17\beta G$ (B) into transporter-expressing cells. The substrate concentrations of telmisartan and $E_2 17\beta G$ used were 0.1 μM. Squares, triangles, and circles represent the uptake by OATP1B3-, OATP1B1-, and vector-transfected cells. The uptake of telmisartan and $E_2 17\beta G$ was evaluated in the presence and absence of 0.3% HSA, respectively. *, a significant difference ($P < 0.05$) from the uptake by vector-transfected cells. Each point represents the mean ± S.E. of three separate determinations.

(Fig. 3). The K_m and V_{max} values of telmisartan uptake into isolated rat hepatocytes and the protein unbound fraction of telmisartan in the presence of 1% HSA were 21.7 μM, 371 pmol/min/10^6 cells, and 0.018, respectively. Then, the K_m value normalized by the unbound concentration in the incubation media was estimated to be 0.4 μM. To evaluate the nonsaturable uptake of telmisartan, we defined 40 μM telmisartan as an excess concentration resulting from the limited solubility of telmisartan in the incubation media. The uptake of telmisartan into isolated rat hepatocytes was Na^+-independent, indicating that telmisartan is not transported by Na^+-taurocholate cotransporting polypeptide, the uptake by which is Na^+-dependent (Fig. 4A). Furthermore, the uptake of telmisartan was inhibited by digoxin, pravastatin, and taurocholate with the IC_{50} value of 45.3, 58.6, and 300 μM, respectively. In contrast, a high concentration of TEA (1 mM) did not inhibit telmisartan uptake (Fig. 4B). Taurocholate, pravastatin, and digoxin are the substrates and inhibitors of Oatp1a1, 1a4, and 1b2 in rats (Noe et al., 1997; Kouzuki et al., 1999; Tokui et al., 1999; Cattori et al., 2000; Sasaki et al., 2004). It is reported that 100 μM digoxin completely inhibited the Oatp1a4 activity, but at most inhibited Oatp1a1-mediated uptake of digoxin by 70% (Shitara et al., 2002). Based on these results, it appears that telmisartan is taken up

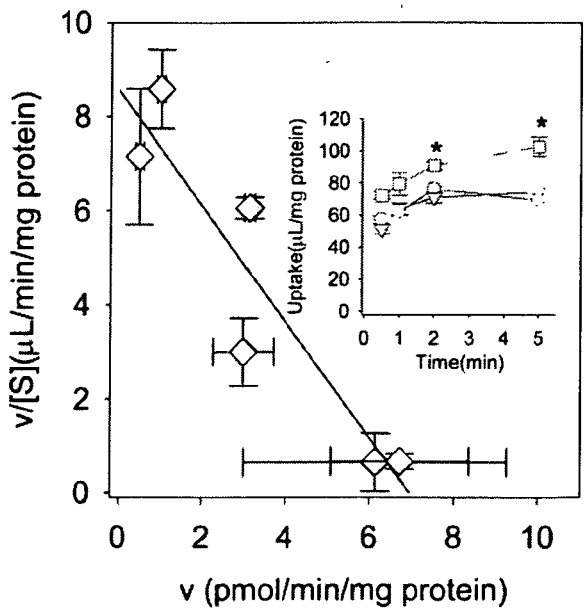

FIG. 6. Time profile and Eadie-Hofstee plot of the uptake of telmisartan into transporter-expressing cells in the absence of HSA. Inset, the substrate concentration used was 0.1 μM. Squares, triangles, and circles represent the uptake by OATP1B3-, OATP1B1-, and vector-transfected cells. The uptake of telmisartan by transporter-expressing cells was measured at a concentration between 0.05 and 10 μM telmisartan in the absence of HSA. The OATP1B3-mediated telmisartan transport was obtained by subtracting the uptake in vector-transfected cells from that in OATP1B3-expressing cells for 5 min. *, a significant difference ($P < 0.05$) from the uptake by vector-transfected cells. Each point represents the mean ± S.E. of three separate determinations.

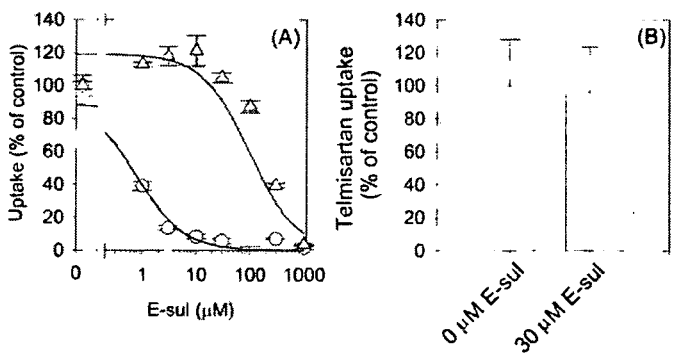

FIG. 7. Inhibitory effect of E-sul on OATP1B1-mediated $E_2 17\beta G$ uptake (A, circle), OATP1B3-mediated CCK-8 uptake (A, triangle), and OATP1B3-mediated telmisartan uptake (B) in the presence of 0.3% HSA. The substrate concentration used was 0.1 μM for all the compounds. The OATP1B1- and OATP1B3-mediated transport was obtained by subtracting the uptake in vector-transfected cells from that in OATP1B1- or OATP1B3-expressing cells for 2 min for $E_2 17\beta G$ or 5 min for CCK-8 and telmisartan. Data are shown as the percentage of the OATP1B1- and OATP1B3-mediated substrate uptake in the absence of E-sul. The solid lines in A represent the fitted curves obtained by nonlinear regression analysis. Each bar and point represents the mean ± S.E. (n = 3).

into rat hepatocytes by Oatp isoforms, and at least Oatp1a4 is involved in the uptake of telmisartan.

Next, to examine which human OATP transporters are involved in the uptake of telmisartan into human hepatocytes, we evaluated the transport properties of telmisartan using HEK293 cells expressing individual OATP and cryopreserved human hepatocytes. In this transport study, we reduced the HSA concentration from 1% to 0.3% in the incubation media because no significant uptake of $E_2 17\beta G$, which is used as a probe substrate for OATP1B1, was detected in OATP1B1-expressing cells in the presence of 1% HSA. Telmisartan could be

TABLE 1

Effect of E-sul on the uptake of telmisartan and $E_2$17β G by cryopreserved human hepatocytes in the presence of 0.3% HSA

The substrate concentration used was 0.1 and 1 μM for telmisartan and $E_2$17β G. Saturable uptake of telmisartan and $E_2$17β G into cryopreserved human hepatocytes was determined after the subtraction of nonsaturable uptake (evaluated as the uptake clearance of the respective compounds in the presence of 40 μM telmisartan and 200 μM $E_2$17β G). In parentheses is the percentage of the saturable uptake of telmisartan and $E_2$17β G in the absence of inhibitor.

E-sul	HH-OCF		HH-094		HH-MYO	
	Telmisartan	$E_2$17βG	Telmisartan	$E_2$17βG	Telmisartan	$E_2$17βG
	μl/min/10⁶ cells		*μl/min/10⁶ cells*		*μl/min/10⁶ cells*	
0 μM	48.5 ± 3.6	5.66 ± 1.1	42.0 ± 1.7	1.85 ± 0.72	16.8 ± 5.3	2.01 ± 0.62
30 μM	63.9 ± 11	1.50 ± 0.75	42.2 ± 0.41	1.03 ± 0.76	18.1 ± 3.7	0.38 ± 0.45
	(131%)	(26.6%)	(100%)	(55.8%)	(108%)	(19.0%)

taken up by OATP1B3 but not by OATP1B1 (Fig. 5A). Because the transporter-mediated uptake of telmisartan in the presence of HSA was not high enough to evaluate the saturation kinetics, we investigated the saturable uptake of telmisartan in the absence of HSA. The K_m and V_{max} values of telmisartan uptake by OATP1B3 in the absence of HSA were 0.81 μM and 6.7 pmol/min/mg protein, respectively (Fig. 6). This K_m value was almost comparable with that in isolated rat hepatocytes normalized by the unbound concentration of telmisartan in the incubation media. Telmisartan was taken up into cryopreserved human hepatocytes in a saturable manner. Considering that telmisartan was taken up by OATP1B3, but not by OATP1B1, the uptake of telmisartan seems to be mediated by OATP1B3. To confirm the minor contribution of OATP1B1 to the hepatic uptake of telmisartan, we planned to perform an inhibition study using OATP1B1- and OATP1B3-selective inhibitor. From our analyses, E-sul inhibited OATP1B1-mediated $E_2$17βG uptake with an IC_{50} value of 0.8 μM, whereas E-sul did not inhibit OATP1B3-mediated CCK-8 uptake up to 30 μM (Fig. 7A). These results confirmed that 30 μM E-sul can selectively inhibit the OATP1B1-mediated uptake. On the other hand, CCK-8 inhibited both OATP1B1- and OATP1B3-mediated $E_2$17βG uptake with IC_{50} value of 6.79 ± 0.59 and 14.6 ± 2.2 μM, respectively, indicating that CCK-8 cannot be used as a selective inhibitor for OATP1B3 as reported previously (Nozawa et al., 2003). The uptake of telmisartan into OATP1B3-expressing cells and cryopreserved human hepatocytes was not inhibited by 30 μM E-sul (Fig. 7B; Table 1). On the contrary, 30 μM E-sul inhibited more than half of $E_2$17βG uptake in all the batches of cryopreserved human hepatocytes (Table 1). Hirano et al. (2004) have reported that the uptake of $E_2$17βG in human hepatocytes is mediated mainly by OATP1B1. These results suggest that telmisartan is transported into cryopreserved human hepatocytes by OATP1B3 rather than OATP1B1.

In a previous study, the ratio of the relative expression level of OATP1B1 and OATP1B3 in cryopreserved human hepatocytes to that in expression systems, determined by Western blot analysis, was 1.79 and 0.96, respectively (Hirano et al., 2004). In human liver, OATP2B1 is also expressed on the basolateral membrane (Kullak-Ublick et al., 2001). We checked that telmisartan was significantly taken up into OATP1B3- and OATP2B1-expressing HEK293 cells (2.6 ± 0.4 and 1.7 ± 0.9 μl/5 min/mg protein, respectively). The ratio of the protein expression level of OATP2B1 in human hepatocytes to that in our expression systems was less than 0.2 (Hirano et al., 2006). Therefore, it is suggested that the contribution of OATP2B1 to the hepatic uptake of telmisartan into human hepatocytes is at most one-fifth that of OATP1B3.

In general, it is accepted that OATP1B1 is responsible for the hepatic uptake of several compounds. Hirano et al. (2004) have shown that pitavastatin and $E_2$17βG are taken up mainly via OATP1B1. However, a recent report suggested that fexofenadine, an H_1-receptor antagonist, is transported by OATP1B3 rather than OATP1B1 (Shimizu et al., 2005). Moreover, in the case of valsartan, which is in the same therapeutic class as telmisartan, the contribution of OATP1B1 and OATP1B3 to its hepatic uptake is estimated to be almost similar (Yamashiro et al., 2006). Therefore, the relative contribution of OATP1B1 and OATP1B3 to the hepatic uptake of organic anions depends on the substrate properties and chemical structures, and we cannot a priori decide which transporters are responsible for hepatic uptake without using dedicated experiments for estimating the contribution of each proposed transporter.

The C_{max} value of telmisartan increases disproportionately with the dose (10–160 mg). In clinical situations, 160/25 mg/day telmisartan/hydrochlorothiazide combination therapy is approved for the treatment of hypertension in the United States. The C_{max} values of telmisartan after single and multiple 160-mg doses were 3.0 and 5.6 μM, respectively (Stangier et al., 2000b). Considering that 99.5% of the telmisartan in blood is bound to plasma proteins (Stangier et al., 2000b), the unbound concentration of telmisartan is estimated to be 0.015 and 0.028 μM. These values are more than 20 times lower than the K_m value of telmisartan uptake by OATP1B3 obtained in this study. In addition, to avoid the false-negative prediction of the contribution of OATP1B3 to its nonlinear pharmacokinetics, we calculated the maximum unbound concentration of telmisartan at the inlet to the liver ($I_{in,\ max,\ u}$) to be 0.12 μM after multiple 160-mg doses using an established method (Ito et al., 1998). However, the K_m value of telmisartan uptake by OATP1B3 is still more than 5 times higher than the $I_{in,\ max,\ u}$ of telmisartan. If the conventional assumption applies, in which only the unbound drug can interact with OATP1B3, the saturation of OATP1B3-mediated telmisartan uptake seems to have a minor effect on the nonlinear increase of C_{max} and AUC over the clinical dose range. Furthermore, a large interindividual variability in the plasma profile of telmisartan has been observed in clinical situations (Stangier et al., 2000a,c). Letschert et al. (2004) have reported two naturally occurring mutations in the *SLCO1B3* gene that cause a substrate-dependent functional change in OATP1B3. The genetic polymorphisms in OATP1B3 may be one of the reasons for the interindividual variability of the pharmacokinetics of telmisartan. In addition, the glucuronidation process of telmisartan and hepatobiliary transport of telmisartan glucuronide may also affect its interindividual variability, and further quantitative analyses in each process will be needed.

In conclusion, we have shown that telmisartan is taken up into human hepatocytes by OATP1B3 rather than by OATP1B1. In addition, these findings support and further extend the important role of OATP1B3 in overall hepatic elimination of some drugs.

References

Abe T, Kakyo M, Tokui T, Nakagomi R, Nishio T, Nakai D, Nomura H, Unno M, Suzuki M, Naitoh T, et al. (1999) Identification of a novel gene family encoding human liver-specific organic anion transporter LST-1. *J Biol Chem* **274**:17159–17163.

Cattori V, Hagenbuch B, Hagenbuch N, Stieger B, Ha R, Winterhalter KE, and Meier PJ (2000)

Identification of organic anion transporting polypeptide 4 (Oatp4) as a major full-length isoform of the liver-specific transporter-1 (rlst-1) in rat liver. *FEBS Lett* **474**:242–245.
Faber KN, Muller M, and Jansen PL (2003) Drug transport proteins in the liver. *Adv Drug Deliv Rev* **55**:107–124.
Hagenbuch B and Meier PJ (2003) The superfamily of organic anion transporting polypeptides. *Biochim Biophys Acta* **1609**:1–18.
Hedner T (1999) Management of hypertension: the advent of a new angiotensin II receptor antagonist. *J Hypertens Suppl* **17**:S21–S25.
Hirano M, Maeda K, Shitara Y, and Sugiyama Y (2004) Contribution of OATP2 (OATP1B1) and OATP8 (OATP1B3) to the hepatic uptake of pitavastatin in humans. *J Pharmacol Exp Ther* **311**:139–146.
Hirano N, Maeda K, Shitara Y, and Sugiyama Y (2006) Drug-drug interaction between pitavastatin and various drugs via OATP1B1. *Drug Metab Dispos* **34**:1229–1236.
Hsiang B, Zhu Y, Wang Z, Wu Y, Sasseville V, Yang WP, and Kirchgessner TG (1999) A novel human hepatic organic anion transporting polypeptide (OATP2). Identification of a liver-specific human organic anion transporting polypeptide and identification of rat and human hydroxymethylglutaryl-CoA reductase inhibitor transporters. *J Biol Chem* **274**:37161–37168.
Ismair MG, Stieger B, Cattori V, Hagenbuch B, Fried M, Meier PJ, and Kullak-Ublick GA (2001) Hepatic uptake of cholecystokinin octapeptide by organic anion-transporting polypeptides OATP4 and OATP8 of rat and human liver. *Gastroenterology* **121**:1185–1190.
Ito K, Iwatsubo T, Kanamitsu S, Ueda K, Suzuki H, and Sugiyama Y (1998) Prediction of pharmacokinetic alterations caused by drug-drug interactions: metabolic interaction in the liver. *Pharmacol Rev* **50**:387–412.
Kok LD, Siu SS, Fung KP, Tsui SK, Lee CY, and Waye MM (2000) Assignment of liver-specific organic anion transporter (SLC22A7) to human chromosome 6 bands p21.2→p21.1 using radiation hybrids. *Cytogenet Cell Genet* **88**:76–77.
Konig J, Cui Y, Nies AT, and Keppler D (2000a) A novel human organic anion transporting polypeptide localized to the basolateral hepatocyte membrane. *Am J Physiol* **278**:G156–G164.
Konig J, Cui Y, Nies AT, and Keppler D (2000b) Localization and genomic organization of a new hepatocellular organic anion transporting polypeptide. *J Biol Chem* **275**:23161–23168.
Kouzuki H, Suzuki H, Ito K, Ohashi R, and Sugiyama Y (1999) Contribution of organic anion transporting polypeptide to uptake of its possible substrates into rat hepatocytes. *J Pharmacol Exp Ther* **288**:627–634.
Kullak-Ublick GA, Ismair MG, Stieger B, Landmann L, Huber R, Pizzagalli F, Fattinger K, Meier PJ, and Hagenbuch B (2001) Organic anion-transporting polypeptide B (OATP-B) and its functional comparison with three other OATPs of human liver. *Gastroenterology* **120**:525–533.
Letschert K, Keppler D, and Konig J (2004) Mutations in the SLCO1B3 gene affecting the substrate specificity of the hepatocellular uptake transporter OATP1B3 (OATP8) *Pharmacogenetics* **14**:441–452.
Noe B, Hagenbuch B, Stieger B, and Meier PJ (1997) Isolation of a multispecific organic anion and cardiac glycoside transporter from rat brain. *Proc Natl Acad Sci USA* **94**:10346–10350.
Nozawa T, Tamai I, Sai Y, Nezu J, and Tsuji A (2003) Contribution of organic anion transporting polypeptide OATP-C to hepatic elimination of the opioid pentapeptide analogue [D-Ala2, D-Leu5]-enkephalin. *J Pharm Pharmacol* **55**:1013–1020.
Oliverio MI and Coffman TM (1997) Angiotensin-II-receptors: new targets for antihypertensive therapy. *Clin Cardiol* **20**:3–6.
Ries UJ, Mihm G, Narr B, Hasselbach KM, Wittneben H, Entzeroth M, van Meel JC, Wienen W, and Hauel NH (1993) 6-Substituted benzimidazoles as new nonpeptide angiotensin II receptor antagonists: synthesis, biological activity and structure-activity relationships. *J Med Chem* **36**:4040–4051.
Sasaki M, Suzuki H, Aoki J, Ito K, Meier PJ, and Sugiyama Y (2004) Prediction of in vivo biliary clearance from the in vitro transcellular transport of organic anions across a double-transfected Madin-Darby canine kidney II monolayer expressing both rat organic anion transporting polypeptide 4 and multidrug resistance associated protein 2. *Mol Pharmacol* **66**:450–459.
Shimizu M, Fuse K, Okudaira K, Nishigaki R, Maeda K, Kusuhara H, and Sugiyama Y (2005) Contribution of OATP (organic anion-transporting polypeptide) family transporters to the hepatic uptake of fexofenadine in humans. *Drug Metab Dispos* **33**:1477–1481.
Shitara Y, Li AP, Kato Y, Lu C, Ito K, Itoh T, and Sugiyama Y (2003) Function of uptake transporters for taurocholate and estradiol 17beta-D-glucuronide in cryopreserved human hepatocytes. *Drug Metab Pharmacokinet* **18**:33–41.
Shitara Y, Sugiyama D, Kusuhara H, Kato Y, Abe T, Meier PJ, Itoh T, and Sugiyama Y (2002) Comparative inhibitory effects of different compounds on rat oatp1 (slc21a1)- and Oatp2 (Slc21a5)-mediated transport. *Pharm Res (NY)* **19**:147–153.
Stangier J, Schmid J, Turck D, Switek H, Verhagen A, Peeters PA, van Marle SP, Tamminga WJ, Sollie FA, and Jonkman JH (2000a) Absorption, metabolism and excretion of intravenously and orally administered [^{14}C]telmisartan in healthy volunteers. *J Clin Pharmacol* **40**:1312–1322.
Stangier J, Su CA, and Roth W (2000b) Pharmacokinetics of orally and intravenously administered telmisartan in healthy young and elderly volunteers and in hypertensive patients. *J Int Med Res* **28**:149–167.
Stangier J, Su CA, Schondorfer G, and Roth W (2000c) Pharmacokinetics and safety of intravenous and oral telmisartan 20 mg and 120 mg in subjects with hepatic impairment compared with healthy volunteers. *J Clin Pharmacol* **40**:1355–1364.
Tamai I, Nezu J, Uchino H, Sai Y, Oku A, Shimane M, and Tsuji A (2000) Molecular identification and characterization of novel members of the human organic anion transporter (OATP) family. *Biochem Biophys Res Commun* **273**:251–260.
Tokui T, Nakai D, Nakagomi R, Yawo H, Abe T, and Sugiyama Y (1999) Pravastatin, an HMG-CoA reductase inhibitor, is transported by rat organic anion transporting polypeptide, oatp2. *Pharm Res (NY)* **16**:904–908.
Vavricka SR, Van Montfoort J, Ha HR, Meier PJ, and Fattinger K (2002) Interactions of rifamycin SV and rifampicin with organic anion uptake systems of human liver. *Hepatology* **36**:164–172.
Wienen W, Entzeroth M, van Meel JCA, Stangier J, Busch U, Ebner T, Schmid J, Lehmann H, Matzek K, Kempthorne-Rawson J, et al. (2000) A review on telmisartan: a novel long-acting angiotensin II-receptor antagonist. *Cardiovasc Drug Rev* **18**:127–156.
Yamaoka K, Tanigawara Y, Nakagawa T, and Uno T (1981) A pharmacokinetic analysis program (multi) for microcomputer. *J Pharmacobio-Dyn* **4**:879–885.
Yamashiro W, Maeda K, Hirouchi M, Adachi Y, Hu Z, and Sugiyama Y (2006) Involvement of transporters in the hepatic uptake and biliary excretion of valsartan, a selective antagonist of the angiotensin II AT1-receptor, in humans. *Drug Metab Dispos* **34**:1247–1254.
Yamazaki M, Suzuki H, Hanano M, Tokui T, Komai T, and Sugiyama Y (1993) Na(+)-independent multispecific anion transporter mediates active transport of pravastatin into rat liver. *Am J Physiol* **264**:G36–G44.

Address correspondence to: Dr. Yuichi Sugiyama, Department of Molecular Pharmacokinetics, Graduate School of Pharmaceutical Sciences, The University of Tokyo, 7-3-1 Hongo, Bunkyo-ku, Tokyo 113-0033, Japan. E-mail: sugiyama@mol.f.u-tokyo.ac.jp

0090-9556/06/3409-1575–1581$20.00
DRUG METABOLISM AND DISPOSITION
Copyright © 2006 by The American Society for Pharmacology and Experimental Therapeutics
DMD 34:1575–1581, 2006

Vol. 34, No. 9
8748/3132909
Printed in U.S.A.

Inhibition of Bile Acid Transport across Na^+/Taurocholate Cotransporting Polypeptide (SLC10A1) and Bile Salt Export Pump (ABCB 11)-Coexpressing LLC-PK1 Cells by Cholestasis-Inducing Drugs

Sachiko Mita, Hiroshi Suzuki, Hidetaka Akita,[1] Hisamitsu Hayashi, Reiko Onuki, Alan F. Hofmann, and Yuichi Sugiyama

Graduate School of Pharmaceutical Sciences, The University of Tokyo, Tokyo, Japan (S.M., H.S., H.A., H.H., R.O., Y.S.); and Department of Medicine, University of California, La Jolla, California (A.H.)

Received December 2, 2005; accepted June 5, 2006

ABSTRACT:

Vectorial transport of bile acids across hepatocytes is a major driving force for bile flow, and bile acid retention in the liver causes hepatotoxicity. The basolateral and apical transporters for bile acids are thought to be targets of drugs that induce cholestasis. Previously, we constructed polarized LLC-PK1 cells that express both a major bile acid uptake transporter human Na^+/taurocholate cotransporting polypeptide (SLC10A1) (NTCP) and the bile acid efflux transporter human bile salt export pump (ABCB 11) (BSEP) and showed that monolayers of such cells can be used to characterize vectorial transcellular transport of bile acids. In the present study, we investigated whether cholestasis-inducing drugs could inhibit bile acid transport in such cells. Because fluorescent substrates allow the development of a high-throughput screening method, we examined the transport by NTCP and BSEP of fluorescent bile acids as well as taurocholate. The aminofluorescein-tagged bile acids, chenodeoxycholylglycylamidofluorescein and cholylglycylamidofluorescein, were substrates of both NTCP and BSEP, and their basal-to-apical transport rates across coexpressing cell monolayers were 4.3 to 4.5 times those of the vector control, although smaller than for taurocholate. The well known cholestatic drugs, rifampicin, rifamycin SV, glibenclamide, and cyclosporin A, reduced the basal-to-apical transport and the apical efflux clearance of taurocholate across NTCP- and BSEP-coexpressing cell monolayers. Further analysis indicated that the drugs inhibited both NTCP and BSEP. Our study suggests that such coexpressing cells can provide a useful system for the identification of inhibitors of these two transport systems, including potential drug candidates.

Hepatotoxic adverse effects, often indicated by cholestasis, are a concern for every drug, and severe hepatotoxicity may cause a drug to be withdrawn from the market. Biliary excretion of bile acids is one of the principal driving forces for bile formation by generating an osmotic driving force favoring influx of water and electrolytes through the paracellular space (Wheeler et al., 1968; Wheeler, 1972). The transcellular transport is mediated by transporter proteins located on the sinusoidal (basolateral) and canalicular (apical) membranes of hepatocytes (Meier and Stieger, 2002; Trauner and Boyer, 2003). The basolateral Na^+/taurocholate cotransporting polypeptide (NTCP/SLC10A1) transports bile acids from the space of Disse into hepatocytes (Hagenbuch et al., 1991; Boyer et al., 1994). Human NTCP accepts most physiological bile acids and some organic anions, such as estrone-3-sulfate and bromosulfophthalein (Meier et al., 1997). Sodium-independent uptake of bile acids is carried out by members of the organic anion-transporting polypeptide family, such as rat Oatp1a1 and human OATP1B1. Although there are several carrier proteins capable of transporting bile acids, much evidence suggests, at least in the rodent, that NTCP-mediated transport accounts for a large part of the total bile acid uptake (Wolkoff and Cohen, 2003). At the canalicular membrane, the efflux of bile acids by the bile salt export pump (BSEP/ABCB11) mediates concentrative excretion (Boyer et al., 1994; Gerloff et al., 1998; Noe et al., 2002). Mutations of BSEP in humans causes progressive familial intrahepatic cholestasis type II, a fatal condition (Strautnieks et al., 1998).

One mechanism for cholestasis is thought to be inhibition of hepatocyte transport systems for bile acids and other organic anions by

This study was supported by a Grant-in-Aid for Scientific Research on Priority Areas Epithelial Vectorial Transport 12144201, a Grant-in-Aid for Center of Excellence (COE) from The Ministry of Education, Culture, Sports, Science and Technology of Japan, and National Institutes of Health Grant DK 64891 at University of California, San Diego.

[1] Current affiliation: Graduate School of Pharmaceutical Sciences, Hokkaido University, Sapporo, Japan.

Article, publication date, and citation information can be found at http://dmd.aspetjournals.org.
doi:10.1124/dmd.105.008748.

ABBREVIATIONS: NTCP, Na^+/taurocholate cotransporting polypeptide (SLC10A1); BSEP, bile salt export pump (ABCB 11); CGamF, cholylglycylamidofluorescein; CamF, cholylamidofluorescein; CDCGamF, chenodeoxycholylglycylamidofluorescein; NBD, 7-nitrobenz-2-oxa-1,3-diazol-4-yl; UDC-L-NBD, ursodeoxycholyl-(N-ε-NBD)-lysine; 7β-NBD-NCT, 7β-NBD-cholyltaurine; PS, permeability-surface area product; LLC-NTCP/BSEP, NTCP- and BSEP-coexpressing LLC-PK1 cells; LLC-NTCP, NTCP-expressing LLC-PK1 cells.

drugs. The inhibitory effects of such drugs on the uptake and efflux of bile acids have been studied using isolated and primary cultured hepatocyte or canalicular membrane vesicles (Kukongviriyapan and Stacey, 1991), as well as the isolated perfused liver (Bolder et al., 1999). Recently, NTCP and BSEP, which generate bile salt-dependent bile flow, have been shown to be possible target molecules for cholestatic drugs (Kim et al., 1999; Stieger et al., 2000; Akita et al., 2001; Bohan and Boyer, 2002).

Previously, we constructed NTCP- and BSEP-coexpressing LLC-PK1 cells as an in vitro model of the vectorial transcellular transport of bile acids in hepatocytes (Mita et al., 2006). This approach is useful for the screening of choleretic bile acids, which are good substrates of these transporters. A second use of this system is to identify inhibitors of these transporters which might have cholestatic effects in vivo. The method should also be useful for defining structure-transport activity relationships of bile acids. In the present study, we assessed the inhibitory effects of cholestasis-inducing drugs on transport across coexpressing cells with the aim of developing a screening system for cholestatic compounds. We compared the transport of fluorescent bile acid derivatives with that of taurocholate in the hope that such fluorescent compounds would be efficiently transported and thereby permit the development of a high-throughput screening method for detecting the inhibitory effects of drug candidates.

Materials and Methods

Chemicals. [^{3}H]Taurocholic acid (2 Ci/mmol) was purchased from PerkinElmer Life Sciences (Boston, MA). Unlabeled taurocholic acid was obtained from Sigma Chemical Co. (St. Louis, MO). Unlabeled cholic acid was purchased from Wako Pure Chemicals Industries, Ltd. (Osaka, Japan). Unlabeled ursodeoxycholic acid, tauroursodeoxycholic acid, and glycoursodeoxycholic acid were kindly provided by Mitsubishi Pharma (Osaka, Japan). Fluorescent bile acids [cholylglycylamidofluorescein (CGamF), cholylamidofluorescein (CamF), chenodeoxycholylglycylamidofluorescein (CDCGamF), ursodeoxycholyl-(Nε-NBD)-lysine (UDC-L-NBD), and 7β-NBD-cholyltaurine (7β-NBD-NCT)] were synthesized in the laboratory of Alan F. Hofmann as described previously (Sorscher et al., 1992; Holzinger et al., 1998). The following compounds were obtained from Sigma-Aldrich (St. Louis, MO): cyclosporin A, rifampicin, rifamycin SV, and glibenclamide. All other chemicals used were commercially available and of reagent grade.

Cell Culture and Transfection. Human NTCP- and human BSEP-expressing LLC-PK1 cells were established and maintained as described previously (Mita et al., 2006). Briefly, parental LLC-PK1 cells were grown in M199 media (Invitrogen, Carlsbad, CA) supplemented with 10% fetal bovine serum and 1% antibiotic-antimycotic (Invitrogen; 100 U/ml penicillin, 100 μg/ml streptomycin, 0.25 μg/ml amphotericin B) at 37°C under 5% CO_2. Full-length human NTCP cDNA was subcloned into pcDNA3.1 (Invitrogen) and transfected into LLC-PK1 cells with FuGENE 6 (Roche Diagnostics Corporation, Indianapolis, IN) according to the manufacturer's instructions. Transfectants expressing NTCP were selected with G418 (800 μg/ml) and the clone with the highest NTCP activity was screened by the uptake activity for taurocholate. The BD Adeno-X Adenoviral Expression System (BD Biosciences, Palo Alto, CA) was used to establish the recombinant adenovirus encoding human BSEP (Hayashi et al., 2005). Forty-eight hours before each experiment, LLC-PK1 cells were infected by the recombinant adenoviruses or control viruses containing green fluorescent protein at a multiplicity of infection of 100.

Transport Studies. NTCP- or mock-transfected LLC-PK1 cells were seeded on Transwell membrane inserts (pore size of 3 μm; Falcon, Bedford, MA) in 12-well plates at a density of 1.4×10^5 cells per insert for transcellular transport studies, cultured at confluence for 2 days, and infected by recombinant adenovirus containing cDNAs for BSEP or GFP (100 multiplicity of infection). For uptake studies, NTCP- or mock-transfected LLC-PK1 cells were seeded on 12-well plates and cultured without viral infection. Cells were harvested 48 h after infection, and expression of NTCP was induced by 10 mM sodium butyrate for 24 h (Cui et al., 1999). To evaluate the integrity of the monolayer, transepithelial electrical resistance was measured using a Millicell-ERS (Millipore Corp., Bedford, MA). The monolayers' transepithelial electrical resistances before the experiments were 200 to 300 Ω cm^2. Then, cells were washed with transport buffer (118 mM NaCl, 23.8 mM $NaHCO_3$, 4.83 mM KCl, 0.96 mM KH_2PO_4, 1.20 mM $MgSO_4$, 12.5 mM HEPES, 5 mM glucose, and 1.53 mM $CaCl_2$ adjusted to pH 7.4). Subsequently, ^{3}H-labeled taurocholate or fluorescent bile acids were added to the transport buffer in the basal compartment (950 μl) for transcellular transport studies or 12-well plates for uptake studies. After the times indicated, the amount of substrates in the opposite apical compartment was measured by the radioactivity for taurocholate, or by the absorbance at 490 nm for fluorescent bile acids using a Microplate Spectrophotometer (Molecular Devices, Sunnyvale, CA). Potential inhibitors were added to both apical and basal compartments 30 min before the transport study. The accumulated radioactivity in the cell was determined at the end of the experiments by lysing the cells with 500 μl of 0.2 N NaOH and measuring the radioactivity in the cell lysates. Aliquots (50 μl) of cell lysate were used to determine protein concentrations by the method of Lowry et al. (1951) with bovine serum albumin as a standard. The apparent intracellular concentration of taurocholate (C_{cell}) was determined by assuming that the cellular volume per milligram of cellular protein was 4 μl.

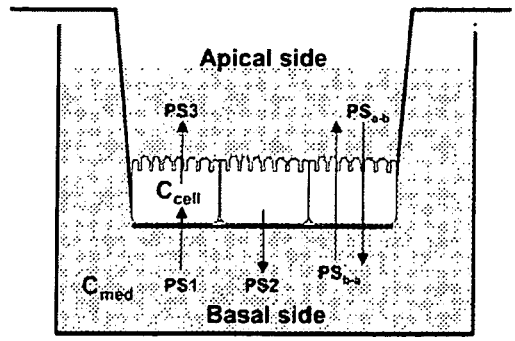

FIG. 1. Schematic diagram illustrating transcellular transport across LLC-PK1 monolayers. PS_{b-a} (μl/min/mg protein) is the PS product for the basal-to-apical clearance defined for the ligand concentration in the medium [C_{med} (pmol/μl)]. PS1 (μl/min/mg protein) is the PS product for the influx of ligand across the basal membrane, which is defined for C_{med}. PS3 (μl/min/mg protein) is the PS product for the efflux of ligand across the apical membrane, which is defined for the ligand concentration in the cells [C_{cell} (pmol/μl)]. PS2 (μl/min/mg protein) is the PS product for the efflux of ligand across the basal membrane from the cell to the basal compartment, which is defined for C_{cell}.

Data Analysis. The kinetic parameters were defined as follows: PS_{b-a} (μl/min/mg protein) is the permeability-surface area product (PS) for the basal-to-apical clearance defined for the ligand concentration in the medium [C_{med} (pmol/μl)] (Fig. 1). PS1 (μl/min/mg protein) is the PS product for the influx of ligand across the basal membrane, which is defined for C_{med}; PS3 (μl/min/mg protein) is the PS product for the efflux of ligand across the apical membrane, which is defined for the ligand concentration in the cells [C_{cell} (pmol/μl)]; and PS2 (μl/min/mg protein) is the PS product for the efflux of ligand across the basal membrane from the cell to the basal compartment, which is defined for C_{cell}. PS_{b-a} is given as a hybrid parameter consisting of PS1, PS2, and PS3 (Mita et al., 2005): $PS_{b-a} = PS1 \cdot PS3/(PS2 + PS3)$.

In this study, PS_{b-a} and PS3 of taurocholate were calculated as follows: $PS_{b-a} = V_{apical}/C_{med}$ and $PS3 = V_{apical}/C_{cell}$, where V_{apical} (pmol/min/mg protein) is the increasing velocity of taurocholate in the apical compartment. V_{apical} was determined by analyzing the transcellular transport for 1 h. Since the amount of taurocholate transported increased linearly as a function of time over the 2-h period and the intracellular concentration was constant during the incubation periods (Mita et al., 2006), we hypothesized that the initial transport velocity could be determined from the slope over the period 0 to 1 h.

Results

Transcellular Transport of Fluorescent Bile Acids. To identify a good substrate of NTCP and BSEP for the functional probe in the inhibition study, the basal-to-apical transport clearance (PS_{b-a}) of taurocholate and fluorescent bile acids across NTCP- and BSEP-coexpressing LLC-PK1 cells (LLC-NTCP/BSEP) was compared

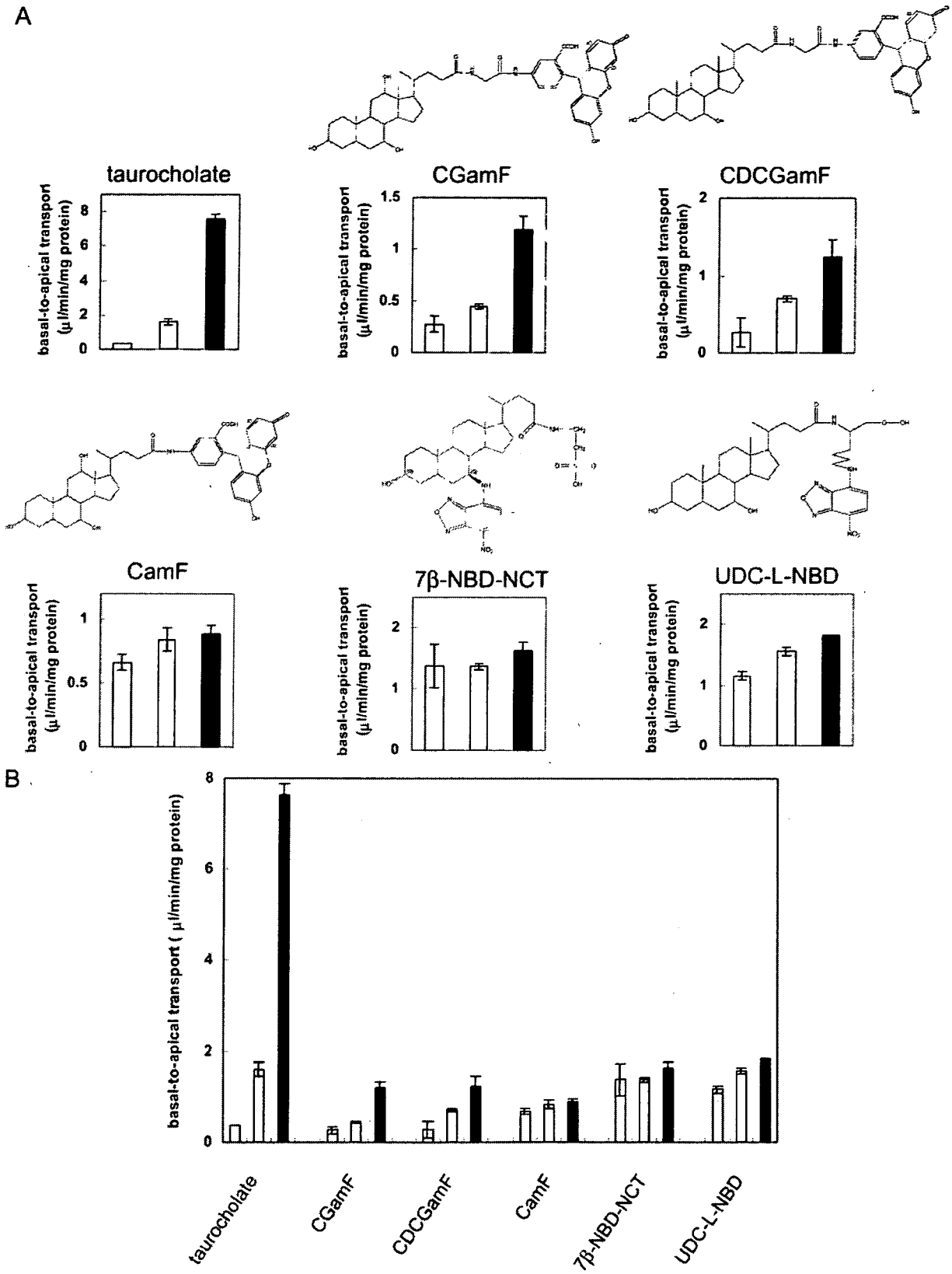

FIG. 2. Transcellular transport of labeled and fluorescent bile acids across NTCP- and BSEP-coexpressing LLC-PK1 cells. [^{3}H]Taurocholate (1 μM), CGamF, CamF, CDCGamF, UDC-L-NBD, and 7β-NBD-NCT (10 μM) across the LLC-PK1 cell monolayers were determined. Open, hatched, and closed bars represent the basal-to-apical transcellular transport across the control (LLC), LLC-NTCP, and LLC-NTCP/BSEP monolayers, respectively. Vertical bars represent the S.E. of three determinations. At the bottom is a graph in which the transcellular transport data are expressed on the same scale.

TABLE 1

Transcellular transport of labeled and fluorescent bile acids across NTCP and BSEP coexpressing LLC-PK1 cells

Data are expressed as mean ± S.E.

	Basal-to-Apical Transport		Ratio (NTCP/BSEP/Control)
	LLC-PK1 (control)	LLC-NTCP/ BSEP	
	μl/min/mg protein		
Taurocholate	0.36 ± 0.00	7.62 ± 0.26	20.94
CGamF	0.28 ± 0.08	1.19 ± 0.13	4.32
CDCGamF	0.27 ± 0.18	1.24 ± 0.22	4.61
CamF	0.66 ± 0.06	0.89 ± 0.07	1.33
7β-NBD-NCT	1.38 ± 0.35	1.63 ± 0.13	1.18
UDC-L-NBD	1.16 ± 0.07	1.83 ± 0.00	1.58

(Figs. 1 and 2; Table 1). The PS_{b-a} values of [^{3}H]taurocholate (1 μM), and CDCGamF and CGamF (10 μM), in LLC-NTCP/BSEP were significantly greater than those in control LLC-PK1 cells and NTCP-expressing LLC-PK1 (LLC-NTCP) cells, indicating that these bile acids are good substrates of BSEP. In contrast, for CamF, UDC-L-NBD (10 μM), and 7β-NBD-NCT (10 μM), transport by NTCP and BSEP was barely detectable.

The value of PS_{b-a} in LLC-NTCP/BSEP was the highest when [^{3}H]taurocholate was used. The absolute PS_{b-a} value of all the fluorescent bile acids was less than ⅙ that of [^{3}H] taurocholate. The ratio of the PS_{b-a} value of LLC-NTCP/BSEP to that of LLC-NTCP was 4.8-fold for [^{3}H]taurocholate, 2.6-fold for CGamF, and 1.8-fold for CDCGamF (Fig. 2, bottom graph). These results indicate that taurocholate is a better substrate for the subsequent inhibition studies. Furthermore, labeled compounds are better tools for measuring the intracellular content of the compounds, which is important for this study because it is needed to calculate the efflux clearance across the apical membrane (PS3).

Inhibitory Effects of a Series of Cholestasis-Inducing Drugs. Next, the inhibitory effect of cholestasis-inducing drugs on the basal-to-apical transport clearance PS_{b-a} of taurocholate was examined (Fig. 3). PS_{b-a} was reduced by 100 μM rifampicin and rifamycin SV to 50% of the control level, and 10 μM glibenclamide reduced it to 70% (Fig. 3A). The intracellular concentration (C_{cell}) of taurocholate was determined for each compound at the end of the experiment (Fig. 3B). The C_{cell} of taurocholate was increased by 100 μM rifampicin to 160% of that of control cells (no inhibitor added). However, 100 μM rifamycin caused a 10% reduction in the apparent cellular concentration of taurocholate and 10 μM glibenclamide led to a 30% reduction in C_{cell} compared with control cells. Calculation of the efflux clearance across the apical membrane PS3 using the measured C_{cell} showed that 100 μM rifampicin, rifamycin SV, and glibenclamide produced a 70%, 44%, and 63% inhibition of PS3, respectively, indicating that the drugs inhibited the efflux of taurocholate by BSEP located in the apical membrane (Fig. 3C). When the efflux process is the only target of inhibition, C_{cell} should be increased by the drugs compared with untreated LLC-NTCP/BSEP cells. However, as mentioned above, C_{cell} was reduced by rifamycin SV and glibenclamide. This means that not only BSEP but also NTCP was inhibited in this experiment as far as rifamycin SV and glibenclamide were concerned. Of course, from these data, we cannot exclude the possibility that inhibition of NTCP is also involved in the case of rifampicin. A 100 μM concentration of captopril and cimetidine did not affect the transport and C_{cell} of taurocholate significantly (Fig. 3, A–C).

Kinetics of the Inhibition by Cyclosporin A. To evaluate the inhibition kinetics involved in the transcellular transport when both the uptake and efflux processes are affected, cyclosporin A, an inhibitor of both NTCP and BSEP, was also examined (Fig. 4). The basal-to-apical transport clearance PS_{b-a} of taurocholate was inhibited by cyclosporin A (and its metabolites) with a K_i value of 1.0 ± 0.2 (μM) (Fig. 4A). The intracellular concentration C_{cell} determined at the end of each experiment was also reduced by cyclosporin A, suggesting that uptake of taurocholate by NTCP was inhibited by cyclosporin A treatment. The inhibition of the uptake process was confirmed by evaluating the inhibitory effect of cyclosporin A on the uptake of taurocholate into only NTCP-expressing LLC-PK1 cells. The K_i value was determined as 0.27 ± 0.06 (μM) (Fig. 4C). At the same time, the calculated PS3 showed a reduction depending on the concentration of cyclosporin A, probably because of inhibition of BSEP by cyclosporin A (and/or its metabolites) (Fig. 4B). These results showed that both uptake and efflux processes are affected by 1 to 10 μM cyclosporin A.

Discussion

In the present study, we assessed the inhibitory effects of cholestasis-inducing drugs on bile acid transport across LLC-NTCP/BSEP cells. Our hope was to develop a rapid screening system for drugs that inhibit these transporters.

Initially, we focused on the fluorescent bile acids as a probe of NTCP and BSEP function and investigated whether they were substrates of NTCP and BSEP using LLC-NTCP/BSEP. The fluorescent derivatives of bile acids used in this study were originally synthesized for the functional analysis of bile salt transport systems in isolated hepatocytes, immortalized cell lines derived from hepatocytes, or in vivo (Holzinger et al., 1998; Cantz et al., 2000). Direct demonstration of the transport of these bile acids via NTCP or BSEP has not yet been carried out, although sodium-dependent uptake for CGamF has been observed (Maglova et al., 1995).

Basal-to-apical transport across LLC-NTCP/BSEP was observed in a rank order of taurocholate > CGamF > CDCGamF, and no significant transport was observed for UDC-L-NBD, CamF, and 7β-NBD-NCT (Fig. 2). This order was similar to that of the maximum output rate of the bile acids in an isolated liver perfusion study: taurocholate 22.7 > CGamF 14.1 > CamF 7.7 > UDC-L-NBD 1.1 (nmol/g liver/min) (Holzinger et al., 1998). This result supports the hypothesis that the transport of fluorescent derivatives of cholic acid in hepatocytes is mainly mediated by NTCP and BSEP, and showed that our in vitro system can reflect the physiological function of these transporters as far as transcellular transport is concerned. As for UDC-L-NBD, although uptake by LLC-NTCP inhibited by taurocholate was observed using fluorescent microscopy (data not shown), no significant transcellular transport across LLC-NTCP/BSEP was observed. This might be because of the nature of this bile salt, which is sequestered in the cells (Holzinger et al., 1998; Cantz et al., 2000). Nonetheless, fluorescent bile acids were transported in this system. Better fluorescent bile acids that will be transported as efficiently as taurocholate will make excellent tools for high-throughput screening.

Inhibition of BSEP by cholestasis-inducible drugs is one of the most frequently reported mechanisms of drug-induced cholestasis (Bohan and Boyer, 2002). Among such drugs, rifampicin, rifamycin SV, glibenclamide, and cyclosporin A (Stieger et al., 2000; Byrne et al., 2002) were used in this study. As shown in Fig. 3, PS3, the efflux clearance that reflects the function of BSEP, was reduced by all the drugs examined. The concentration needed for 50% inhibition of PS3 is between 10 and 100 μM for rifampicin and glibenclamide and approximately 100 μM for rifamycin SV. The reported K_i values for the inhibition of taurocholate uptake into human BSEP-expressing membrane vesicles are 31 μM for rifamycin SV and 31 μM for glibenclamide (Byrne et al., 2002). For rifampicin, only the K_i value of 12 μM for rat Bsep is available (Stieger et al., 2000). Compared

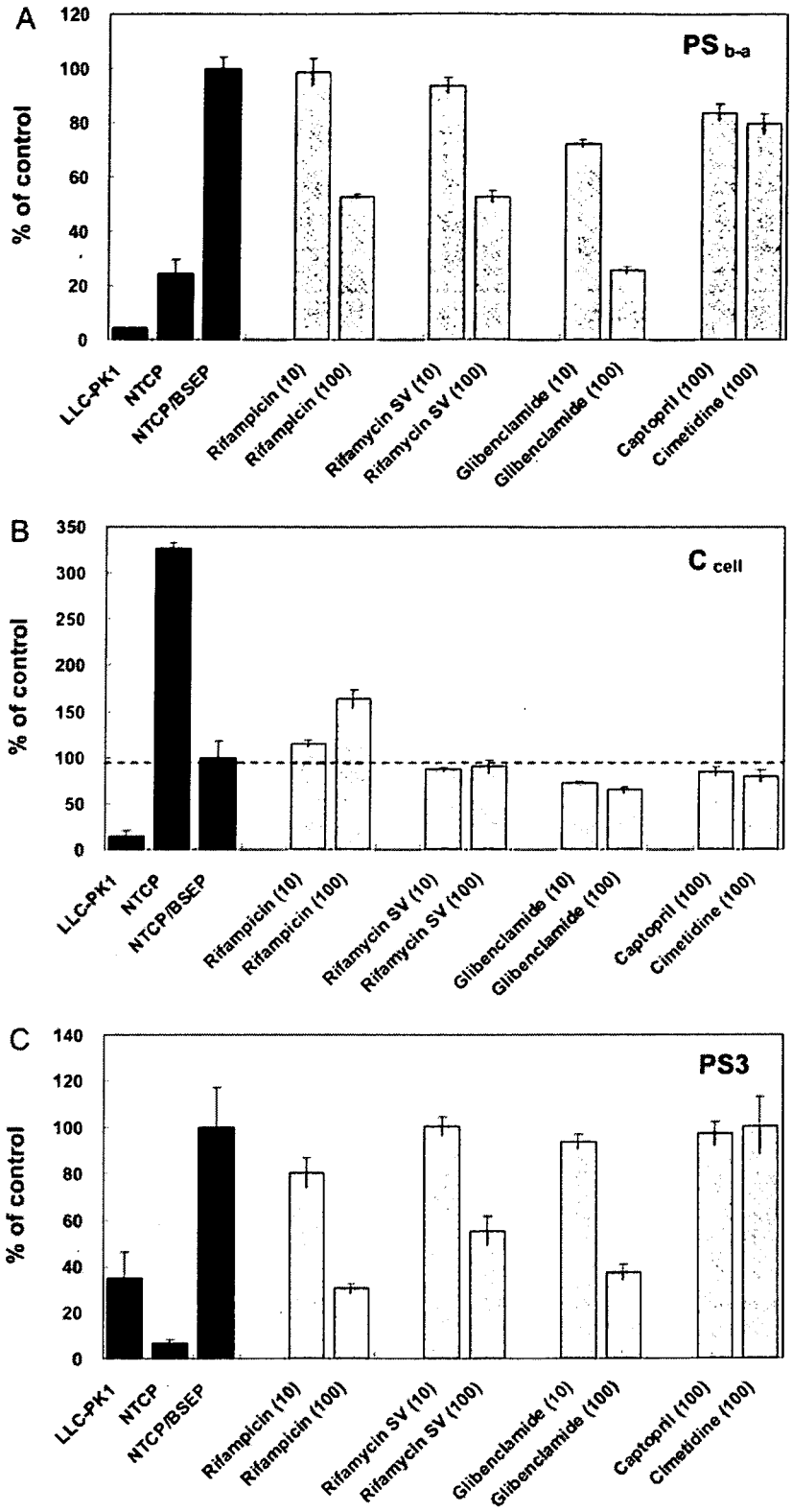

FIG. 3. Inhibitory effects of cholestasis-inducing drugs on the transport of taurocholate across NTCP- and BSEP-coexpressing LLC-PK1 cells. Basal-to-apical transport clearance PS_{b-a} (A), intracellular concentration C_{cell} (B), and apical efflux clearance PS3 (C) of taurocholate in LLC-PK1, LLC-NTCP, and LLC-NTCP/BSEP cell monolayers were determined at 60 min (closed bars). Inhibitory effects of 10 or 100 μM concentrations of various drugs on LLC-NTCP/BSEP were studied (open and hatched bars). The drugs were added to the apical and basal compartment 30 min before applying taurocholate.

with these values, the inhibitory concentration was higher in our LLC-NTCP/BSEP cells than in other studies that used vesicles. One possible explanation for this is that the protein unbound concentrations of the drugs in cytoplasm are lower than in the medium because the drugs may not penetrate the plasma membrane efficiently and the drugs may also bind to intracellular proteins.

Inhibition of BSEP in the transcellular transport of taurocholate should be accompanied by an increase in the intracellular concentration of taurocholate. However, the increase was observed only in the case of rifampicin. This means that rifamycin SV and glibenclamide also inhibited NTCP-mediated uptake at the same time. Recently, it has been reported that 100 μM rifampicin or rifamycin SV can reduce

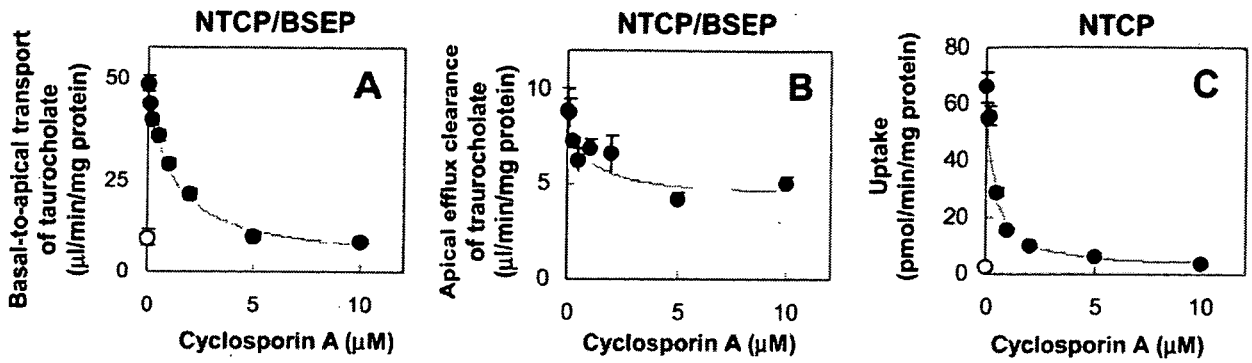

FIG. 4. Inhibition of the transport of taurocholate by cyclosporin A. Various concentrations of cyclosporin A were added to the apical and basal compartment of LLC-NTCP/BSEP (A and B). After 30 min, the inhibitory effects of cyclosporin A (closed circles) and an excess (500 μM) of taurocholate (open circle) on the basal-to-apical transport of [^{3}H]taurocholate (1 μM) for 1 h across LLC-NTCP/BSEP cell monolayers were studied (A). Apical efflux clearance PS3 of taurocholate was calculated versus the intracellular concentration of taurocholate determined at the end of the experiments (B). The inhibitory effects of cyclosporin A (closed circles) and an excess (500 μM) of taurocholate (open circle) on the uptake of [^{3}H]taurocholate (1 μM) for 1 min into LLC-NTCP cells were studied (C).

the uptake of taurocholate by rat Ntcp to 60% of the total uptake (Fattinger et al., 2000). However, in this study, after incubation with 100 μM rifampicin and rifamycin SV, the reduction in C_{cell} was not as much as 60%. An increase by rifampicin and only a slight decrease by rifamycin SV were observed (Fig. 3). If we hypothesize there is no species difference in the inhibitory effect of these drugs between humans and rats, this result indicates that the inhibition of NTCP and BSEP balanced each other.

Captopril and cimetidine are reported to cause cholestasis (Mohiud-din and Lewis, 2004). However, their interactions with bile acid transporters have not been reported [cimetidine does not have a significant inhibitory effect on BSEP (Wang et al., 2003)], and other pathways are postulated as a possible mechanism. Corresponding to this, both captopril and cimetidine did not affect the transcellular transport and C_{cell} of taurocholate at 100 μM (Fig. 3, A–C).

The inhibitory effect of cyclosporin A, an inhibitor of both NTCP and BSEP, was also examined as well as the inhibition kinetics of the transcellular transport when both the uptake and efflux processes are affected (Fig. 4). The basal-to-apical transport clearance $PS_{b\text{-}a}$ was inhibited with a K_i value of 1.0 ± 0.2 (μM). The efflux clearance PS3 was inhibited depending on the medium concentration of cyclosporin A. Although estimation of the exact K_i value is difficult, it appeared to be close to the reported K_i value for the inhibition of the uptake of taurocholate into human BSEP-expressing membrane vesicles by cyclosporin A (9.5 μM) (Byrne et al., 2002)

The question that we must consider here is to what extent inhibition of the uptake and efflux process affects the net transcellular transport. It was estimated that the K_i value for the inhibitory effect of cyclosporin A on the uptake of taurocholate into human NTCP-expressing LLC-PK1 cells was 0.27 ± 0.06 (μM) (Fig. 4). This value is similar to the K_i value for $PS_{b\text{-}a}$, which suggests that the inhibition of $PS_{b\text{-}a}$ reflects the inhibition of the uptake process mediated by NTCP. Although we do not know whether NTCP or BSEP is important for the cyclosporin A-induced cholestasis in physiological situations, the result of this study and the following aspects support the importance of NTCP. The transcellular transport clearance can be expressed as the hybrid of each transmembrane transport clearance as described under *Data Analysis*: $PS_{b\text{-}a} = PS1 \cdot PS3/(PS2 + PS3)$. If the efflux clearance across the apical membrane, PS3, is far greater than that across the basal membrane, PS2, $PS_{b\text{-}a}$ is nearly equal to PS1. Thus, inhibition of the uptake process, PS1, can lead to inhibition of transcellular transport more easily than inhibition of the efflux process, PS3. The effect of inhibition of the uptake and/or efflux process on the net transcellular transport is simulated in Fig. 5. The ratio of PS2:PS3 is substituted by the measured value in the isolated rat liver perfusion studies: PS3, 69.2 ± 6.3 (μl/min/g liver); PS2, 8.4 ± 0.6 (μl/min/g liver) (Akita et al., 2002). If the efficacy of the inhibitory effect of the drug is similar for the uptake and efflux processes, inhibition of uptake is more effective than that of efflux as far as the net transcellular transport is concerned.

BSEP has been extensively studied as a target molecule of drug-induced cholestasis because it plays a role in the regulation of the concentration of bile acids in hepatocytes. Inhibition of BSEP leads to an intracellular accumulation of bile acids, resulting in cellular damage because of their cytotoxic effects. However, there should be some cases where the inhibition of NTCP plays a major role in drug-induced cholestasis, considering the importance of the uptake process in the overall transcellular transport of bile acids as described above. Cyclosporin A-induced cholestasis may be one of those. The plasma bile salt concentration was increased in rats after administration of 10 mg/kg cyclosporin A (Stone et al., 1987), indicating that cyclosporin A inhibits the uptake of bile acids from the portal blood into hepato-

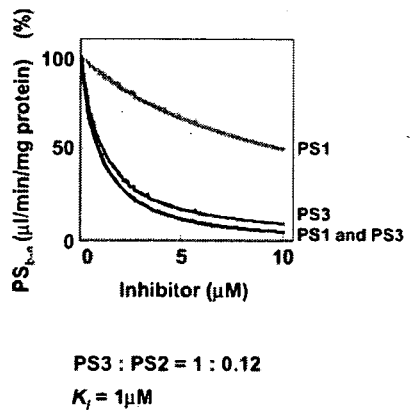

FIG. 5. Simulation of the inhibitory effect of the uptake and/or efflux process on the net basal-to-apical transport of bile taurocholate across hepatocytes. The basal-to-apical clearance $PS_{b\text{-}a}$ of taurocholate across hepatocytes was calculated in the cases where the influx clearance, PS1, the efflux clearance, PS3, or both were affected by the inhibitor under the following conditions. The K_m values of PS1 and PS3 are = 30 μM and 6 μM, respectively, according to the reported K_m values for rat Ntcp and rat Bsep (Schroeder et al., 1998; Hagenbuch et al., 1991; Gerloff et al., 1998; Akita et al., 2001). The unbound concentrations of taurocholate in the basal compartment and the intracellular compartment are smaller than these K_m values (fixed at 1 μM). The inhibition constant K_i for both the influx and efflux clearance is K_i = 1 μM; PS2:PS3 = 1:8.2; $PS_{b\text{-}a} = PS1 \cdot PS3/(PS2 + PS3)$, according to the equation under *Data Analysis*. $PS_{b\text{-}a} = PS1 \cdot PS3/(PS2 + PS3)$. The ratio of PS1:PS2:PS3 is substituted by the measured value (PS1:PS2:PS3 = 1.0:0.7:6.0) in the isolated rat liver perfusion studies cited from Akita et al. (2002).

cytes. Moreover, there was no change in liver histology in the cholestasis caused by cyclosporin A (Kukongviriyapan and Stacey, 1991), suggesting that the cytotoxicity brought about by intracellular bile acids here is not very severe. These facts indicate the importance of the inhibition of NTCP, at least in the case of cyclosporin A-induced cholestasis.

In conclusion, LLC-NTCP/BSEP cells were used for the detection of the inhibitory effect of drugs on NTCP and/or BSEP, although the quantitative evaluation of the inhibitory effect on BSEP appears to be difficult at the present time, compared with transport studies using membrane vesicles. Furthermore, to predict the effect of drugs under physiological conditions, we must consider the drug metabolites, which sometimes significantly inhibit BSEP (Funk et al., 2001). Because there is only a minor quantity of hepatic enzymes involved in drug metabolism in LLC-PK1 cells (Gonzalez and Tarloff, 2004), the inhibitory effects observed in this study are speculated to be those produced by drugs in their unchanged forms. The additional expression of such enzymes and uptake transporters of drugs, such as OATP1B1 and OATP1B3, will provide a more useful tool for quantitative measurement of the inhibitory effect on BSEP.

References

Akita H, Suzuki H, Ito K, Kinoshita S, Sato N, Takikawa H, and Sugiyama Y (2001) Characterization of bile acid transport mediated by multidrug resistance associated protein 2 and bile salt export pump. *Biochim Biophys Acta* **1511**:7–16.

Akita H, Suzuki H, and Sugiyama Y (2002) Sinusoidal efflux of taurocholate correlates with the hepatic expression level of Mrp3. *Biochem Biophys Res Commun* **299**:681–687.

Bohan A and Boyer JL (2002) Mechanisms of hepatic transport of drugs: implications for cholestatic drug reactions. *Semin Liver Dis* **22**:123–136.

Bolder U, Trang NV, Hagey LR, Schteingart CD, Ton-Nu HT, Cerre C, Elferink RP, and Hofmann AF (1999) Sulindac is excreted into bile by a canalicular bile salt pump and undergoes a cholehepatic circulation in rats. *Gastroenterology* **117**:962–971.

Boyer JL, Ng OC, Ananthanarayanan M, Hofmann AF, Schteingart CD, Hagenbuch B, Stieger B, and Meier PJ (1994) Expression and characterization of a functional rat liver Na+ bile acid cotransport system in COS-7 cells. *Am J Physiol* **266**:G382–387.

Byrne JA, Strautnieks SS, Mieli-Vergani G, Higgins CF, Linton KJ, and Thompson RJ (2002) The human bile salt export pump: characterization of substrate specificity and identification of inhibitors. *Gastroenterology* **123**:1649–1658.

Cantz T, Nies AT, Brom M, Hofmann AF, and Keppler D (2000) MRP2, a human conjugate export pump, is present and transports fluo 3 into apical vacuoles of Hep G2 cells. *Am J Physiol* **278**:G522–G531.

Cui Y, Konig J, Buchholz JK, Spring H, Leier I, and Keppler D (1999) Drug resistance and ATP-dependent conjugate transport mediated by the apical multidrug resistance protein, MRP2, permanently expressed in human and canine cells. *Mol Pharmacol* **55**:929–937.

Fattinger K, Cattori V, Hagenbuch B, Meier PJ, and Stieger B (2000) Rifamycin SV and rifampicin exhibit differential inhibition of the hepatic rat organic anion transporting polypeptides, Oatp1 and Oatp2. *Hepatology* **32**:82–86.

Funk C, Ponelle C, Scheuermann G, and Pantze M (2001) Cholestatic potential of troglitazone as a possible factor contributing to troglitazone-induced hepatotoxicity: in vivo and in vitro interaction at the canalicular bile salt export pump (Bsep) in the rat. *Mol Pharmacol* **59**:627–635.

Gerloff T, Stieger B, Hagenbuch B, Madon J, Landmann L, Roth J, Hofmann AF, and Meier PJ (1998) The sister of P-glycoprotein represents the canalicular bile salt export pump of mammalian liver. *J Biol Chem* **273**:10046–10050.

Gonzalez RJ and Tarloff JB (2004) Expression and activities of several drug-metabolizing enzymes in LLC-PK1 cells. *Toxicol In Vitro* **18**:887–894.

Hagenbuch B, Stieger B, Foguet M, Lubbert H, and Meier PJ (1991) Functional expression cloning and characterization of the hepatocyte Na+/bile acid cotransport system. *Proc Natl Acad Sci USA* **88**:10629–10633.

Hayashi H, Takada T, Suzuki H, Akita H, and Sugiyama Y (2005) Two common PFIC2 mutations are associated with the impaired membrane trafficking of BSEP/ABCB11. *Hepatology* **41**:916–924.

Holzinger F, Schteingart CD, Ton-Nu HT, Cerre C, Steinbach JH, Yeh HZ, and Hofmann AF (1998) Transport of fluorescent bile acids by the isolated perfused rat liver: kinetics, sequestration, and mobilization. *Hepatology* **28**:510–520.

Kim RB, Leake B, Cvetkovic M, Roden MM, Nadeau J, Walubo A, and Wilkinson GR (1999) Modulation by drugs of human hepatic sodium-dependent bile acid transporter (sodium taurocholate cotransporting polypeptide) activity. *J Pharmacol Exp Ther* **291**:1204–1209.

Kukongviriyapan V and Stacey NH (1991) Chemical-induced interference with hepatocellular transport. Role in cholestasis. *Chem-Biol Interact* **77**:245–261.

Lowry OH, Rosebrough NJ, Farr AL, and Randall RJ (1951) Protein measurement with the Folin phenol reagent. *J Biol Chem* **193**:265–2751.

Maglova LM, Jackson AM, Meng XJ, Carruth MW, Schteingart CD, Ton-Nu HT, Hofmann AF, and Weinman SA (1995) Transport characteristics of three fluorescent conjugated bile acid analogs in isolated rat hepatocytes and couplets. *Hepatology* **22**:637–647.

Meier PJ, Eckhardt U, Schroeder A, Hagenbuch B, and Stieger B (1997) Substrate specificity of sinusoidal bile acid and organic anion uptake systems in rat and human liver. *Hepatology* **26**:1667–1677.

Meier PJ and Stieger B (2002) Bile salt transporters. *Annu Rev Physiol* **64**:635–661.

Mita S, Suzuki H, Akita H, Hayashi H, Onuki R, Hofmann AF, and Sugiyama Y (2006) Vectorial transport of unconjugated and conjugated bile salts by monolayers of LLC-PK1 cells doubly transfected with human NTCP and BSEP or with rat Ntcp and Bsep. *Am J Physiol* **290**:G550–556.

Mita S, Suzuki H, Akita H, Stieger B, Meier PJ, Hofmann AF, and Sugiyama Y (2005) Vectorial transport of bile salts across MDCK cells expressing both rat Na+-taurocholate cotransporting polypeptide and rat bile salt export pump. *Am J Physiol* **288**:G159–G167.

Mohi-ud-din R and Lewis JH (2004) Drug- and chemical-induced cholestasis. *Clin Liver Dis* **8**:95–132.

Noe J, Stieger B, and Meier PJ (2002) Functional expression of the canalicular bile salt export pump of human liver. *Gastroenterology* **123**:1659–1666.

Schroeder A, Eckhardt U, Stieger B, Tynes R, Schteingart CD, Hofmann AF, Meier PJ, and Hagenbuch B (1998) Substrate specificity of the rat liver Na(+)-bile salt cotransporter in Xenopus laevis oocytes and in CHO cells. *Am J Physiol* **274**:G370–G375.

Sorscher S, Lillienau J, Meinkoth JL, Steinbach JH, Schteingart CD, Feramisco J, and Hofmann AF (1992) Conjugated bile acid uptake by Xenopus laevis oocytes induced by microinjection with ileal Poly A+ mRNA. *Biochem Biophys Res Commun* **186**:1455–1462.

Stieger B, Fattinger K, Madon J, Kullak-Ublick GA, and Meier PJ (2000) Drug- and estrogen-induced cholestasis through inhibition of the hepatocellular bile salt export pump (Bsep) of rat liver. *Gastroenterology* **118**:422–430.

Stone BG, Udani M, Sanghvi A, Warty V, Plocki K, Bedetti CD, and Van Thiel DH (1987) Cyclosporin A-induced cholestasis. The mechanism in a rat model. *Gastroenterology* **93**:344–351.

Strautnieks SS, Bull LN, Knisely AS, Kocoshis SA, Dahl N, Arnell H, Sokal E, Dahan K, Childs S, Ling V, et al. (1998) A gene encoding a liver-specific ABC transporter is mutated in progressive familial intrahepatic cholestasis. *Nat Genet* **20**:233–238.

Trauner M and Boyer JL (2003) Bile salt transporters: molecular characterization, function, and regulation. *Physiol Rev* **83**:633–671.

Wang EJ, Casciano CN, Clement RP, and Johnson WW (2003) Fluorescent substrates of sister-P-glycoprotein (BSEP) evaluated as markers of active transport and inhibition: evidence for contingent unequal binding sites. *Pharm Res (NY)* **20**:537–544.

Wheeler HO (1972) Secretion of bile acids by the liver and their role in the formation of hepatic bile. *Arch Intern Med* **130**:533–541.

Wheeler HO, Ross ED, and Bradley SE (1968) Canalicular bile production in dogs. *Am J Physiol* **214**:866–8748.

Wolkoff AW and Cohen DE (2003) Bile acid regulation of hepatic physiology: I. Hepatocyte transport of bile acids. *Am J Physiol* **284**:G175–G179.

Address correspondence to: Yuichi Sugiyama, Department of Molecular Pharmacokinetics, Graduate School of Pharmaceutical Sciences, The University of Tokyo, 7-3-1 Hongo, Bunkyo-ku, Tokyo 113-0033, Japan. E-mail: sugiyama@mol.f.u-tokyo.ac.jp

0090-9556/06/3407-1247-1254$20.00
DRUG METABOLISM AND DISPOSITION
Copyright © 2006 by The American Society for Pharmacology and Experimental Therapeutics
DMD 34:1247-1254, 2006

Vol. 34, No. 7
8938/3122648
Printed in U.S.A.

INVOLVEMENT OF TRANSPORTERS IN THE HEPATIC UPTAKE AND BILIARY EXCRETION OF VALSARTAN, A SELECTIVE ANTAGONIST OF THE ANGIOTENSIN II AT1-RECEPTOR, IN HUMANS

Wakaba Yamashiro, Kazuya Maeda, Masakazu Hirouchi, Yasuhisa Adachi, Zhuohan Hu, and Yuichi Sugiyama

Graduate School of Pharmaceutical Sciences, the University of Tokyo, Tokyo, Japan (W.Y., K.M., M.H., Y.S.); Daiichi Pure Chemicals Co., Ltd., Tokyo, Japan (Y.A.); and Research Institute for Liver Diseases, Shanghai, China (Z.H.)

Received December 13, 2005; accepted April 18, 2006

ABSTRACT:

Valsartan is a highly selective angiotensin II AT1-receptor antagonist for the treatment of hypertension. Valsartan is mainly excreted into the bile in unchanged form. Because valsartan has an anionic carboxyl group, we hypothesized that a series of organic anion transporters could be involved in its hepatic clearance. In this study, to identify transporters that mediate the hepatic uptake and biliary excretion of valsartan and estimate the contribution of each transporter to the overall hepatic uptake and efflux, we characterized its transport using transporter-expressing systems, human cryopreserved hepatocytes, and Mrp2-deficient Eisai hyperbilirubinemic rats (EHBRs). Valsartan was significantly taken up into organic anion-transporting polypeptide (OATP) 1B1 (OATP2/OATP-C)- and OATP1B3 (OATP8)-expressing HEK293 cells. We also observed saturable uptake into human hepatocytes. Based on our estimation, the relative contribution of OATP1B1 to the uptake of valsartan in human hepatocytes depends on the batch, ranging from 20 to 70%. Regarding efflux transporters, the ratio of basal-to-apical transcellular transport of valsartan to that in the opposite direction in OATP1B1/MRP2 (multidrug resistance-associated protein 2) double transfected cells was the highest among the three kinds of double transfectants, OATP1B1/MRP2, OATP1B1/multidrug resistance 1, and OATP1B1/breast cancer resistance protein-expressing MDCKII cells. We observed saturable ATP-dependent transport into membrane vesicles expressing human MRP2. We also found that the elimination of intravenously administered valsartan from plasma was markedly delayed, and the biliary excretion was severely impaired in EHBR compared with normal Sprague-Dawley rats. These results suggest that OATP1B1 and OATP1B3 as the uptake transporters and MRP2 as the efflux transporter are responsible for the efficient hepatobiliary transport of valsartan.

Valsartan is an antihypertensive drug acting on angiotensin II AT1 receptors. It has been reported that approximately 70% of the total clearance of valsartan is accounted for by hepatic clearance (Flesch et al., 1997). Valsartan undergoes a minor degree of metabolism involving 4-hydroxylation, whereas 85% of orally administered valsartan is excreted into feces in unchanged form (Waldmeier et al., 1997). Considering that the bioavailability is approximately 40% and the hepatic clearance is much less than the hepatic blood flow (Flesch et al., 1997), most of the drug passing into the bile is in the unmetabolized form. From these facts, valsartan is thought to be mainly excreted into the bile in unchanged form. However, the molecular mechanism of the hepatobiliary transport of valsartan has not been elucidated.

When valsartan is given orally to rats, the hepatic concentration is about 7 to 10 times higher than the plasma concentration, suggesting that valsartan is selectively distributed to the liver (interview form of Diovan tablet). Because valsartan is a hydrophilic compound with a log D value (pH = 7.0) of −0.34 and it has an anionic carboxyl group, it should have difficulty in crossing the plasma membrane. Therefore, a number of organic anion transporters could be involved in the hepatic transport of valsartan.

The organic anion-transporting polypeptide (OATP) family transporters play an important role in the transport of organic anions (Hagenbuch and Meier, 2004). Among them, OATP1B1 (OATP-C/OATP2) and OATP1B3 (OATP8) are thought to be responsible for the hepatic uptake of several organic anions in humans because of their selective expression in liver and broad substrate specificities (Hagenbuch and Meier, 2004). They can also accept a variety of clinically used drugs, such as 3-hydroxy-3-methylglutaryl CoA reductase inhibitors, rifampin, and methotrexate (Hsiang et al., 1999; Abe

This work was partly supported by Health and Labor Sciences Research Grants from the Ministry of Health, Labor, and Welfare for the Research on Advanced Medical Technology and by Grant-in Aid for Young Scientists B (17790113) from the Ministry of Education, Culture, Sports, Science, and Technology.

Article, publication date, and citation information can be found at http://dmd.aspetjournals.org.

doi:10.1124/dmd.105.008938.

ABBREVIATIONS: OATP, organic anion-transporting polypeptide; AUC, area under the plasma concentration-time curve; BCRP, breast cancer resistance protein; CCK-8, cholecystokinin octapeptide; E_1S, estrone-3-sulfate; $E_2 17\beta G$, estradiol-17β-glucuronide; EHBR, Eisai hyperbilirubinemic rat; MRP2, multidrug resistance-associated protein 2; MDR1, multidrug resistance 1; *PS*, permeability surface; SD, Sprague-Dawley; CL, clearance.

et al., 2001; Nakai et al., 2001; Vavricka et al., 2002; Shitara et al., 2003a; Hirano et al., 2004). OATP2B1 (OATP-B) is also expressed in the basolateral membrane of human liver. Its substrate specificity is relatively narrow compared with OATP1B1 and 1B3, but some of the OATP1B1 and OATP1B3 substrates can also be recognized by OATP2B1 (Tamai et al., 2000; Kullak-Ublick et al., 2001). Conversely, multidrug resistance 1 (MDR1), multidrug resistance-associated protein 2 (MRP2), and breast cancer resistance protein (BCRP) can be involved in the hepatic efflux transport of organic anions (Chandra and Brouwer, 2004).

In general, the substrate specificity of each transporter is very broad and it is often very similar to that of other transporters, suggesting that a substrate can be recognized by multiple transporters. Now we can use human cryopreserved hepatocytes for the evaluation of transporter-mediated uptake. Shitara et al. (2003a) have succeeded in clarifying the importance of OATP1B1-mediated inhibition in the clinical drug-drug interaction between cerivastatin and cyclosporin A from in vitro experiments using human cryopreserved hepatocytes and transporter expression systems.

Hirano et al. (2004) have recently published their methodology for estimating the quantitative contribution of OATP1B1 and OATP1B3 to the hepatic uptake of compounds. In one of their approaches, they calculated the ratio of the uptake clearance of transporter-selective substrates in human cryopreserved hepatocytes to that in transporter-expression systems, and then estimated the hepatic uptake of test compounds mediated by certain transporters by multiplying that ratio by the clearance of the test compounds in transporter-expressing cells. We applied this method to the calculation of the contribution of OATP1B1 and OATP1B3 to the human hepatic uptake. To check the involvement of efflux transporters in the biliary excretion of compounds, Matsushima et al. (2005) have shown that OATP1B1/MDR1, OATP1B1/MRP2, and OATP1B1/BCRP double transfectants can be used for the rapid identification of anionic bisubstrates of OATP1B1 and each efflux transporter by measuring the vectorial transport of substrates across each monolayer. If valsartan is a substrate of OATP1B1, these cell lines should help us to identify which transporters are involved in its biliary excretion in humans.

In this study, we analyzed the involvement and relative contribution of OATP1B1 and OATP1B3 to the hepatic uptake of valsartan using human cryopreserved hepatocytes and transporter-expressing cells and identified the transporters responsible for the biliary excretion of valsartan using double transfectants and transporter-expressing vesicles. We also checked the involvement of MRP2 in the pharmacokinetics of valsartan in vivo using Eisai hyperbilirubinemic rats (EHBR), in which Mrp2 is deficient.

Materials and Methods

Materials. [^{3}H]Valsartan (80.9 Ci/mmol) and unlabeled valsartan were kindly donated by Novartis Pharma K.K. (Basel, Switzerland). [^{3}H]Estradiol-17β-glucuronide ($E_2$17βG) (45 Ci/mmol) and [^{3}H]estrone-3-sulfate (46 Ci/mmol) were purchased from PerkinElmer Life and Analytical Sciences (Boston, MA), and [^{3}H]cholecystokinin octapeptide (CCK-8) (77 Ci/mmol) was purchased from GE Healthcare Bio-Sciences (Buckinghamshire, UK). Unlabeled $E_2$17βG, estrone-3-sulfate, and CCK-8 were purchased from Sigma-Aldrich (St. Louis, MO). All other chemicals were of analytical grade and commercially available.

Cell Culture. Transporter-expressing or vector-transfected HEK293 cells and MDCKII cells were grown in Dulbecco's modified Eagle's medium low glucose (Invitrogen, Carlsbad, CA) supplemented with 10% fetal bovine serum (Sigma, St. Louis, MO), 100 U/ml penicillin, 100 μg/ml streptomycin, and 0.25 μg/ml amphotericin B at 37°C with 5% CO_2 and 95% humidity. LLC-PK1 cells were cultured in Medium 199 (Invitrogen) supplemented with 10% fetal bovine serum (Sigma), 100 U/ml penicillin, and 100 μg/ml streptomycin.

Transport Study Using Transporter Expression Systems. Cells were seeded in 12-well plates coated with poly-L-lysine/poly-L-ornithine at a density of 1.5×10^5 cells/well 72 h before transport assay. For the transport study, the cell culture medium was replaced with culture medium supplemented with 5 mM sodium butyrate 24 h before transport assay to induce the expression of OATP1B1, OATP1B3, or OATP2B1.

The transport study was carried out as described previously (Hirano et al., 2004, 2006). Uptake was initiated by adding Krebs-Henseleit buffer containing radiolabeled and unlabeled substrates after cells had been washed twice and preincubated with Krebs-Henseleit buffer at 37°C for 15 min. The Krebs-Henseleit buffer consisted of 118 mM NaCl, 23.8 mM $NaHCO_3$, 4.8 mM KCl, 1.0 mM KH_2PO_4, 1.2 mM $MgSO_4$, 12.5 mM HEPES, 5.0 mM glucose, and 1.5 mM $CaCl_2$ adjusted to pH 7.4. The uptake was terminated at designated times by adding ice-cold Krebs-Henseleit buffer after removal of the incubation buffer. Then, cells were washed twice with 1 ml of ice-cold Krebs-Henseleit buffer, solubilized in 500 μl of 0.2 N NaOH, and kept overnight at 4°C. Aliquots (500 μl) were transferred to scintillation vials after adding 250 μl of 0.4 N HCl. The radioactivity associated with the cells and incubation buffer was measured in a liquid scintillation counter (LS6000SE; Beckman Coulter, Inc., Fullerton, CA) after adding 2 ml of scintillation fluid (Clear-sol I; Nacalai Tesque, Kyoto, Japan) to the scintillation vials. The remaining 50 μl of cell lysate was used to determine the protein concentration by the method of Lowry et al. (1951) with bovine serum albumin as a standard.

Transport Study Using Human Cryopreserved Hepatocytes. This experiment was performed as described previously (Hirano et al., 2004). Cryopreserved human hepatocytes were purchased from In Vitro Technologies (Baltimore, MD) (lot 094 and OCF) and from the Research Institute for Liver Disease (Shanghai, China) (lot 03-013). Immediately before the study, the hepatocytes (1-ml suspension) were thawed at 37°C, then quickly suspended in 10 ml of ice-cold Krebs-Henseleit buffer and centrifuged (50g) for 2 min at 4°C, followed by removal of the supernatant. This procedure was repeated once more to remove cryopreservation buffer, and then the cells were resuspended in the same buffer to give a cell density of 1.0×10^6 viable cells/ml for the uptake study. The number of viable cells was determined by trypan blue staining. Before the uptake studies, the cell suspensions were prewarmed in an incubator at 37°C for 3 min. The uptake studies were initiated by adding an equal volume of buffer containing labeled and unlabeled substrates to the cell suspension. After incubation at 37°C for 0.5, 2, or 5 min, the reaction was terminated by separating the cells from the substrate solution. For this purpose, an aliquot of 80-μl incubation mixture was collected and placed in a centrifuge tube (450 μl) containing 50 μl of 2 N NaOH under a layer of 100 μl of oil (density, 1.015; a mixture of silicone oil and mineral oil; Sigma-Aldrich), and subsequently, the sample tube was centrifuged for 10 s using a tabletop centrifuge (10,000g; Beckman Microfuge E; Beckman Coulter, Inc.). During this process, hepatocytes passed through the oil layer into the alkaline solution. After an overnight incubation in alkali to dissolve the hepatocytes, the centrifuge tube was cut and each compartment was transferred to a scintillation vial. The compartment containing the dissolved cells was neutralized with 50 μl of 2 N HCl and mixed with scintillation cocktail, and the radioactivity was measured in a liquid scintillation counter.

Transcellular Transport Study Using Double Transfected Cells. The protocol has been described in detail previously (Matsushima et al., 2005). In brief, transfected MDCKII cells were seeded in a Transwell membrane insert (6.5-mm diameter, 0.4-μm pore size; Corning Costar, Cambridge, MA) at a density of 1.4×10^5 cells per well 96 h before the transport study. Among a series of cell lines we used in this experiment, human MDR1, MRP2, and OATP1B1 were stably transfected into MDCKII cells as shown previously (Evers et al., 1998; Matsushima et al., 2005). Human BCRP cDNA was transduced into MDCKII cells by the infection of recombinant adenovirus 48 h before the transport study. The cell culture medium was replaced with culture medium supplemented with 5 mM sodium butyrate 24 h before the transport assay. For uptake studies, cells were washed three times and preincubated with Krebs-Henseleit buffer. The experiment was initiated by replacing the medium at either the apical or the basal side of the cell layer with complete medium containing ^{3}H-labeled and unlabeled valsartan or $E_2$17βG (0.1 μM). The cells were incubated at 37°C and aliquots of medium were taken from each compartment at several time points. Radioactivity in 100 μl of medium was measured in a liquid scintillation counter after addition of 2 ml of scintillation

fluid. At the end of the experiments, the cells were washed three times with 1.5 ml of ice-cold Krebs-Henseleit buffer and solubilized in 500 μl of 0.2 N NaOH. After addition of 100 μl of 1 N HCl, 400-μl aliquots were transferred to scintillation vials. Then, 50-μl aliquots of cell lysate were used to determine protein concentrations by the method of Lowry et al. (1951) with bovine serum albumin as a standard.

Vesicle Transport Assay. The preparation procedure of the membrane vesicles expressing human MRP2 was described previously (Hirouchi et al., 2004). The transport medium (10 mM Tris, 250 mM sucrose, and 10 mM $MgCl_2$, pH 7.4) contained the labeled and unlabeled valsartan, 5 mM ATP, and an ATP-regenerating system (10 mM creatine phosphate and 100 μg/μl creatine phosphokinase). An aliquot of transport medium (15 μl) was mixed rapidly with the vesicle suspension (5 μg of protein in 5 μl). The transport reaction was stopped by the addition of 1 ml of ice-cold buffer containing 250 mM sucrose, 0.1 M NaCl, and 10 mM Tris-HCl buffer (pH 7.4). The stopped reaction mixture was passed through a 0.45-μm HA filter (Millipore Corp., Billerica, MA) and then washed twice with 5 ml of stop solution. The radioactivity retained on the filter was measured in a liquid scintillation counter after the addition of scintillation cocktail. Ligand uptake was normalized in terms of the amount of membrane protein.

In Vivo Pharmacokinetic Study. Male Sprague-Dawley (SD) rats and EHBRs (7–8 weeks old) were purchased from Nippon SLC (Shizuoka, Japan). All animals were maintained under standard conditions with a reverse dark-light cycle and were treated humanely. Food and water were available ad libitum. This study was carried out in accordance with the guidelines provided by the Institutional Animal Care Committee (Graduate School of Pharmaceutical Sciences, The University of Tokyo, Tokyo, Japan). SD rats and EHBRs were anesthetized by inhalation of diethyl ether. The abdomen was opened with a midline incision and the common bile duct was cannulated with a polyethylene tube (Becton Dickinson Primary Care Diagnostics, Sparks, MD). The phosphate-buffered saline containing [^{3}H]valsartan (8 μCi/ml) and unlabeled valsartan (1 mg/ml) was injected into a femoral vein (1 ml/kg body weight). Blood samples were collected from a femoral artery and bile samples were collected in preweighed tubes at designated times. The total radioactivity in plasma and bile samples was measured in a liquid scintillation counter.

Kinetic Analyses of Uptake Transporters. Ligand uptake was expressed as the uptake volume [μl/mg protein], given as the amount of radioactivity associated with the cells [dpm/mg protein] divided by its concentration in the incubation medium [dpm/μl]. Specific uptake was obtained by subtracting the uptake into vector-transfected cells from the uptake into cDNA-transfected cells. Kinetic parameters were obtained using the following equation:

$$v = \frac{V_{max} \cdot S}{K_m + S} + P_{dif} \cdot S \quad (1)$$

where v is the uptake velocity of the substrate (pmol/min/mg protein), S is the substrate concentration in the medium (μM), K_m is the Michaelis constant (μM), V_{max} is the maximum uptake rate (pmol/min/mg protein), and P_{dif} is the nonsaturable uptake clearance (μl/min/mg protein). Fitting was performed by the nonlinear least-squares method using a MULTI program (Yamaoka et al., 1981), and the Damping Gauss-Newton Method algorithm was used for curve fitting. The input data were weighted as the reciprocal of the observed values.

To determine the saturable hepatic uptake clearance in human hepatocytes, we first determined the hepatic uptake clearance ($CL_{(2\ min-0.5\ min)}$) (μl/min/10^6 cells) by calculating the slope of the uptake volume (V_d) (μl/10^6 cells) between 0.5 and 2 min (eq. 2). The saturable component of the hepatic uptake clearance (CL_{hep}) was determined by subtracting $CL_{(2\ min-0.5\ min)}$ in the presence of 100 μM substrate (excess) from that in the presence of 1 μM substrate (tracer quantity) (eq. 3).

$$CL_{(2\ min-0.5\ min)} = \frac{V_{d,2\ min} - V_{d,0.5\ min}}{2 - 0.5} \quad (2)$$

$$CL_{hep} = CL_{(2\ min-0.5\ min),tracer} - CL_{(2\ min-0.5\ min),excess} \quad (3)$$

where $CL_{(2\ min-0.5\ min),\ tracer}$ and $CL_{(2\ min-0.5\ min),\ excess}$ represent the $CL_{(2\ min-0.5\ min)}$ values estimated in the presence of 1 and 100 μM substrate, respectively.

Estimation of the Relative Contribution of Each Transporter to the Hepatic Uptake. This method for estimating the contribution of OATP1B1 and OATP1B3 to the overall hepatic uptake has been used previously (Hirano et al., 2004). In this analysis, estrone-3-sulfate and CCK-8 were chosen as transporter-selective substrates of OATP1B1 and OATP1B3, respectively. The ratio of the uptake clearance of the reference compounds in human hepatocytes to that in the expression system was calculated and defined as $R_{act,\ OATP1B1}$ and $R_{act,\ OATP1B3}$. The uptake clearance mediated by OATP1B1 and OATP1B3 in human hepatocytes was separately calculated by multiplying the uptake clearance of valsartan in transporter-expressing cells ($CL_{OATP1B1,\ test}$ and $CL_{OATP1B3,\ test}$) by $R_{act,\ OATP1B1}$ and $R_{act,\ OATP1B3}$, respectively, as described in the following equations:

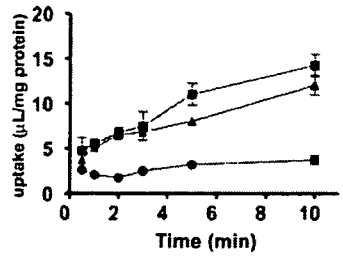

FIG. 1. Time profiles of the uptake of valsartan by OATP1B1- and OATP1B3-expressing HEK293 cells. Squares, triangles, and circles represent the uptake in OATP1B1- and OATP1B3-expressing cells and vector-control cells, respectively. Each point represents the mean ± S.E. (n = 3).

$$R_{act,OATP1B1} = \frac{CL_{Hep,E_1S}}{CL_{OATP1B1,E_1S}} \quad (4)$$

$$R_{act,OATP1B3} = \frac{CL_{Hep,CCK\text{-}8}}{CL_{OATP1B3,CCK\text{-}8}} \quad (5)$$

$$CL_{hep,test,OATP1B1} = CL_{OATP1B1,test} \cdot R_{act,OATP1B1} \quad (6)$$

$$CL_{hep,test,OATP1B3} = CL_{OATP1B3,test} \cdot R_{act,OATP1B3} \quad (7)$$

Kinetic Analyses of Efflux Transporters. The basal-to-apical transcellular clearance (CL_{trans}) was calculated by dividing the steady-state efflux velocity for the transcellular transport (V_{apical}) by the ligand concentration in the incubation buffer on the basal side, whereas the efflux clearance across the apical membrane (PS_{apical}) in double transfected cells was obtained by dividing V_{apical} by the intracellular concentration of ligand at 120 min. In the vesicle transport assay, ATP-dependent transporter-specific uptake was calculated by subtracting the uptake in the presence of AMP from that in the presence of ATP. The saturation kinetics of CL_{trans}, PS_{apical}, and ATP-dependent uptake into vesicles were calculated using eq. 1 by the curve-fitting procedure described above.

Pharmacokinetic Analysis. The plasma concentration-time profile was fitted to a biexponential equation and the $AUC_{0-\infty}$ was estimated by integration up to infinity. The initial distribution volume (V_1) was calculated by dividing the dose by the initial plasma concentration estimated from the fitted biexponential equation. The plasma clearance (CL_p) was calculated as Dose/$AUC_{0-\infty}$. The biliary clearance (CL_{bile}) was calculated as the ratio of the cumulative excreted amount in bile over 120 min to the AUC over 120 min ($AUC_{0-120\ min}$).

Results

Uptake of Valsartan by OATP Transporter-Expressing Cells. Valsartan was significantly taken up into OATP1B1- and OATP1B3-expressing HEK293 cells compared with vector-transfected cells in a time-dependent manner (Fig. 1). The saturation kinetics of valsartan by OATP1B1- and OATP1B3-expressing cells and vector-transfected HEK293 was evaluated by the uptake for 5 min, over which time the uptake of valsartan remained linear, and shown as Eadie-Hofstee plots (Fig. 2). The concentration dependence of the uptake of valsartan could be explained by a one-saturable and one-nonsaturable component. Their kinetic parameters are summarized in Table 1. In contrast,

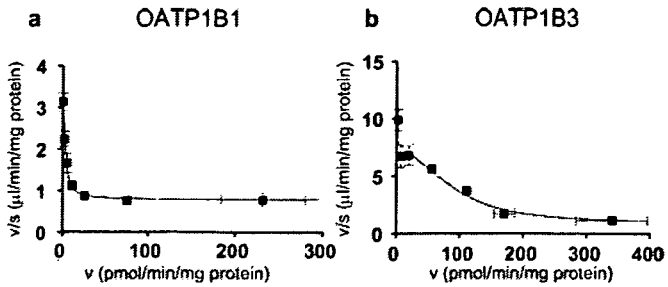

FIG. 2. Eadie-Hofstee plots of the uptake of valsartan by OATP1B1- and OATP1B3-expressing HEK293 cells. The concentration dependence of OATP1B1 (a)- and OATP1B3 (b)-mediated uptake of valsartan is shown as Eadie-Hofstee plots. The uptake of valsartan for 5 min was determined at various concentrations (0.1–300 μM). Each point represents the mean ± S.E. (n = 3).

TABLE 1

Kinetic parameters of the uptake of valsartan by OATP1B1- and OATP1B3-expressing HEK293 cells

Data shown in Fig. 2 were used to determine these parameters calculated by nonlinear regression analysis as described under *Materials and Methods*. Each parameter represents the mean ± computer-calculated S.D.

	K_m	V_{max}	P_{dif}
	μM	*pmol/min/mg protein*	*ml/min/mg protein*
OATP1B1	1.39 ± 0.24	3.85 ± 0.46	0.747 ± 0.022
OATP1B3	18.2 ± 5.9	135 ± 40	0.680 ± 0.223

valsartan was not significantly transported in OATP2B1-expressing HEK293 cells [0.627 ± 0.092 μl/min/mg protein (OATP2B1-expressing HEK293 cells) versus 0.552 ± 0.081 μl/min/mg protein (vector-control cells); mean ± S.E.].

Uptake of Estrone-3-Sulfate, CCK-8, and Valsartan by Human Cryopreserved Hepatocytes. Typical time profiles of the uptake of estrone-3-sulfate, CCK-8, and valsartan in one batch of human hepatocytes (lot OCF) are shown in Fig. 3. The uptake of labeled valsartan by human hepatocytes was inhibited by unlabeled 100 μM valsartan in a concentration-dependent manner (Fig. 4). Time-dependent uptake of all ligands was observed at 1 μM, and this was reduced in the presence of 100 μM unlabeled ligands in all batches of hepatocytes examined in the present study (data not shown). The uptake clearance of these substrates in each batch is listed in Table 2. Based on the data in Table 2, following the method for estimating the contribution of OATP1B1 and OATP1B3 to the overall hepatic uptake described previously (Hirano et al., 2004), we calculated the estimated clearance of valsartan mediated by OATP1B1 and OATP1B3 and the quantitative contribution of these transporters to the hepatic uptake in three batches of human hepatocytes. Our estimation indicated that the relative contribution of OATP1B1 and OATP1B3 depends on the batch of human hepatocytes, ranging from 20% to 70% (as the contribution of OATP1B1) (Table 3).

Transcellular Transport of Valsartan across MDCKII Monolayers. To identify the efflux transporters involved in the biliary excretion of valsartan, we investigated the transcellular transport of valsartan across the MDCKII monolayers expressing uptake and efflux transporters. We could not see any significant vectorial transcellular transport of valsartan in single transfected MDCKII cells expressing OATP1B1, MDR1, MRP2, and BCRP, and vector-transfected control cells. In contrast, as shown in Fig. 5, the basal-to-apical transcellular transport of valsartan in OATP1B1/MRP2 double transfected cells was the largest among three kinds of double transfectants, OATP1B1/MRP2, OATP1B1/MDR1, and OATP1B1/BCRP. In parallel, we also checked the transcellular transport of $E_2$17βG, whose basal-to-apical transport was reported to be observed in three kinds of

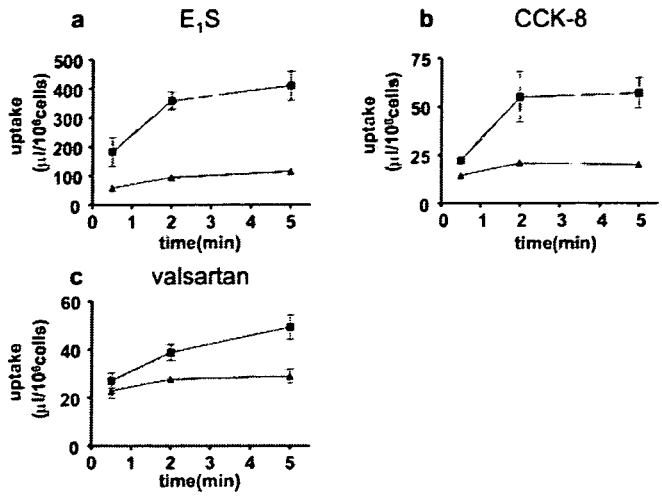

FIG. 3. Typical time profiles of the uptake of estrone-3-sulfate, CCK-8, and valsartan by human hepatocytes (lot OCF). The uptake of estrone-3-sulfate (a), CCK-8 (b), and valsartan (c) for 0.5, 2, and 5 min was determined at two concentrations (squares, 1 μM; triangles, 100 μM) at 37°C. Each point represents the mean ± S.E. (n = 3).

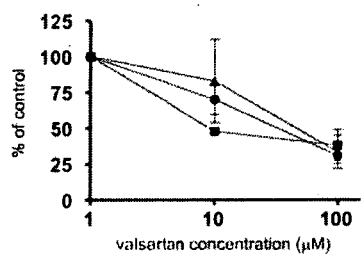

FIG. 4. Concentration dependence of uptake of valsartan by human hepatocytes. The uptake of valsartan for 0.5 and 2 min was determined at three concentrations (1, 10, and 100 μM) at 37°C. The uptake clearance was obtained by subtracting the uptake at 0.5 min from that at 2 min, and the uptake clearance at 1 μM valsartan is defined as 100%. Circles, squares, and triangles represent the uptake in lots OCF, 03-013, and 094, respectively. Each point represents the mean ± S.E. (n = 3).

TABLE 2

Uptake clearance of reference compounds (E_1S and CCK-8) and valsartan in expression systems and human hepatocytes

	Transporter-Expressing Cells		Human Hepatocytes		
	$CL_{OATP1B1}$	$CL_{OATP1B3}$	OCF	094	03-013
	μl/min/mg protein		*μl/min/10^6 cells*		
E_1S	84.6		93.0	98.7	45.2
CCK-8		10.3	17.7	71.6	3.65
valsartan	1.56	0.96	3.55	17.1	6.15

double transfectants we tested (Fig. 5, a–c). The basal-to-apical transport of $E_2$17βG was 36, 8.9, and 6.1 times larger than that in the opposite direction in OATP1B1/MRP2, OATP1B1/MDR1, and OATP1B1/BCRP double transfectants, respectively, which is almost comparable to the previous results (Matsushima et al., 2005). Then, we studied the concentration dependence of the transcellular transport of valsartan in OATP1B1/MRP2-expressing cells (Fig. 6a), and the efflux clearance across the apical membrane (PS_{apical}) was determined by measuring the cellular accumulation of valsartan at 120 min (Fig. 6b). The K_m value of transcellular transport of valsartan (27.5 μM) was smaller than that for PS_{apical} (99.0 μM) (Table. 4).

ATP-Dependent Uptake of Valsartan in Human MRP2-Expressing Membrane Vesicles. To confirm that valsartan is a substrate of human MRP2, the time-dependent uptake of [^{3}H]valsartan by

TABLE 3

Contribution of OATP1B1 and OATP1B3 to the hepatic uptake of valsartan in each batch of human hepatocytes

In the column 'Estimated Clearance of Valsartan,' the lower row shows the percentage of OATP1B1- or OATP1B3-mediated uptake clearance relative to the sum of the estimated clearance mediated by OATP1B1 and OATP1B3. The details of this estimation are described under *Materials and Methods*.

Lot	Ratio of Uptake Clearance $CL_{hep}/CL_{transporter}$		Estimated Clearance of Valsartan	
	$R_{act,OATP1B1}$	$R_{act,OATP1B3}$	OATP1B1	OATP1B3
			μl/min/10⁶ cells	
OCF	1.10	1.72	1.72	1.65
			51.0%	49.0%
094	1.17	6.95	1.83	6.67
			21.5%	78.5%
03–013	0.53	0.35	0.827	0.336
			71.1%	28.9%

TABLE 4

Kinetic parameters of the transcellular transport of valsartan in OATP1B1/MRP2 double transfectant

Data shown in Fig. 6 were used to determine these parameters calculated by nonlinear regression analysis as described under *Materials and Methods*. Each parameter represents the mean ± computer-calculated S.D.

	K_m	V_{max}	P_{dif}
	μM	*pmol/min/mg protein*	*ml/min/mg protein*
Transcellular transport	27.5 ± 4.1	164 ± 24	0.937 ± 0.123
PS_{apical}	99.0 ± 51.1	461 ± 275	0.120 ± 0.610

membrane vesicles prepared from MRP2-expressing LLC-PK1 cells was examined. [^{3}H]Valsartan was significantly taken up into the membrane vesicles expressing MRP2 in an ATP-dependent manner (Fig. 7a), and this uptake could be saturated with K_m, V_{max}, and P_{dif} values of 30.4 ± 17.7 μM, 895 ± 578 pmol/min/mg protein, and 8.88 ± 3.05 μl/min/mg protein, respectively.

Pharmacokinetics of Valsartan in SD Rats and EHBRs. After i.v. administration of 1 mg of valsartan per kg of body weight, we compared the plasma concentration and the biliary excretion of valsartan in SD rats and EHBRs. The plasma concentration was significantly higher in EHBRs compared with SD rats (Fig. 8a). After 2 h, 70% of the total radioactivity injected was excreted into bile in SD rats, whereas in EHBRs, only 15% was excreted (Fig. 8b). The pharmacokinetic parameters of valsartan after i.v. administration in SD rats and EHBRs are summarized in Table. 5. The plasma $AUC_{0-\infty}$ of EHBRs was 17 times higher than that of SD rats, and the total body plasma clearance and biliary clearance were markedly decreased in EHBRs to 6% and 2% of control SD rats, respectively.

Discussion

In humans, valsartan is mainly excreted into bile, mostly in the unchanged form without any significant metabolism (Waldmeier et al., 1997). Considering this physicochemical property, we hypothesized that a series of transporters of organic anions could be involved in the hepatic transport of valsartan. Therefore, in this study, we identified transporters that mediate the hepatic uptake and biliary excretion of valsartan in humans.

First, we performed uptake experiments using OATP1B1 and OATP1B3 expression systems. These transporters are thought to be important for the transport of organic anions in human liver because they are selectively expressed in the liver and can accept a wide variety of compounds. We found that valsartan can be taken up via both OATP1B1 and OATP1B3. In contrast, no significant uptake of valsartan was observed in OATP2B1-expressing cells compared with vector-transfected control cells, suggesting that the contribution of

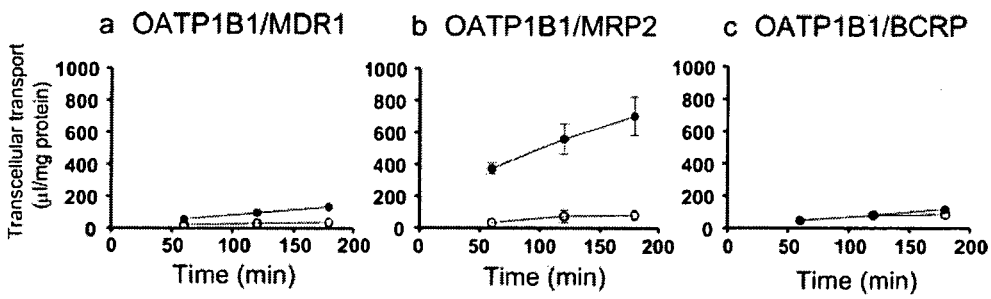

FIG. 5. Time profiles of the transcellular transport of valsartan across MDCKII monolayers expressing transporters. Transcellular transport of valsartan (0.1 μM) across MDCKII monolayers expressing OATP1B1/MDR1 (a), OATP1B1/MRP2 (b), and OATP1B1/BCRP (c) was observed. Open circles and closed circles represent the transcellular transport in the apical-to-basal and basal-to-apical directions, respectively. Each point represents the mean ± S.E. (n = 3).

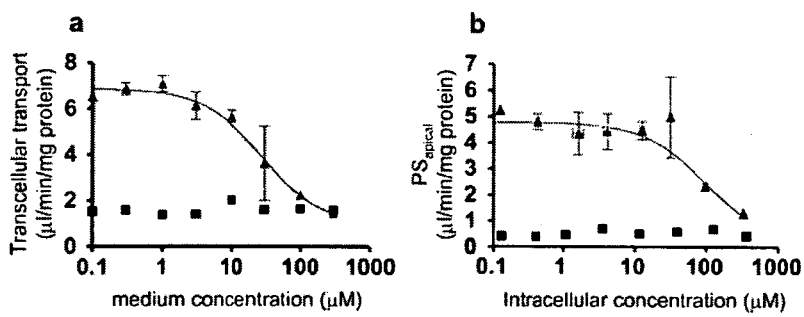

FIG. 6. Concentration dependence of the transcellular clearance (a) and intrinsic clearance across the apical membrane (b) in OATP1B1/MRP2-expressing MDCKII cells. The transcellular transport of valsartan across OATP1B1/MRP2 MDCKII monolayer was observed for 2 h at 37°C (a). The intrinsic clearance for the transport of valsartan across the apical membrane (PS_{apical}) was determined by dividing the transcellular transport velocity of valsartan determined over 2 h by the cellular concentration determined at the end of the experiments (2 h) (b). Triangles and squares represent the transcellular transport across OATP1B1/MRP2 double transfectants and vector-transfected control cells, respectively. Each point represents the mean ± S.E. (n = 3).

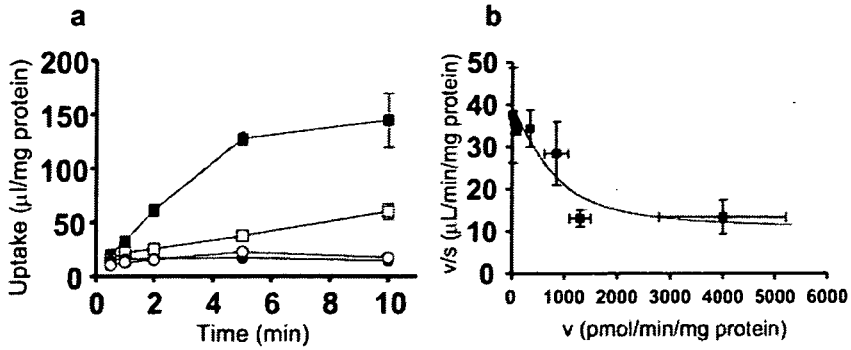

FIG. 7. The ATP-dependent transport of valsartan in MRP2-expressing LLC-PK1 cells. Time profiles for the uptake of valsartan were measured in isolated membrane vesicles prepared from LLC-PK1 cells expressing MRP2 (a). Membrane vesicles were incubated at 37°C with valsartan (0.1 μM) in the medium in the presence of ATP (closed symbols) or AMP (open symbols) for designated periods (0.5, 1, 2, 5, or 10 min). Squares and circles represent the uptake of membrane vesicles expressing MRP2 and control vesicles infected only with adenovirus containing tetracycline-responsive transcriptional activator, respectively. The concentration dependence of MRP2-mediated uptake of valsartan is shown as Eadie-Hofstee plots (b). The uptake of valsartan for 2 min was determined at various concentrations (0.3–300 μM). Each point represents the mean ± S.E. (n = 3).

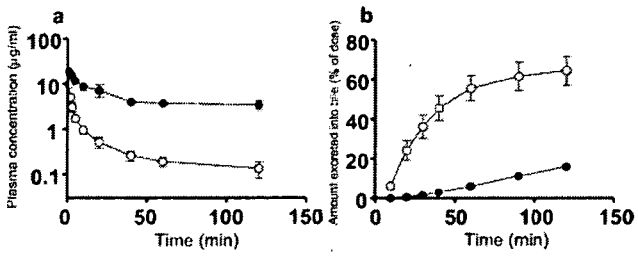

FIG. 8. Biliary elimination of valsartan in male SD rats and EHBRs. Rats were injected with valsartan (1 mg/kg body weight dissolved in phosphate-buffered saline) into a femoral vein after cannulation of the bile duct. The time profiles of the plasma concentration (a) and cumulative biliary excretion (b) of valsartan in SD rats (open circles) and EHBRs (closed circles) are shown. Each point represents the mean ± S.E. (n = 3).

OATP2B1 is negligible as far as hepatic uptake is concerned. To understand the relative importance of OATP1B1 and OATP1B3 in the hepatic uptake of valsartan, we cannot easily compare the uptake clearance of OATP1B1 and OATP1B3 in transporter expression systems because the relative expression level of OATP1B1 and OATP1B3 is different in human hepatocytes and expression systems. To overcome this problem, Hirano et al. (2004) established a methodology for estimating the contribution of OATP1B1 and OATP1B3 to the hepatic uptake of compounds. We used the approach called the relative activity factor (RAF) method (Hirano et al., 2004), in which we use transporter-specific ligands (estrone-3-sulfate for OATP1B1, CCK-8 for OATP1B3). To determine the contribution of transporters, we used three different batches of human hepatocytes prepared from independent donors because Shitara et al. (2003b) reported that there were large interbatch differences in uptake activity in human cryopreserved hepatocytes. Valsartan was taken up by all batches of human hepatocytes in a saturable manner. In the presence of 100 μM valsartan, the time course of the uptake of valsartan was almost flat for 5 min, whereas the uptake of 1 μM valsartan was clearly observed by 2 min, indicating that 100 μM valsartan is enough to saturate the transporter-mediated uptake. This is consistent with our results showing that the K_m values of OATP1B1 and OATP1B3 were much lower than 100 μM. We observed the self-saturation of the uptake of valsartan in human hepatocytes at three concentrations (1, 10, and 100 μM), and the uptake clearance at 10 μM was decreased to half of that at 1 μM (Fig. 4).

According to the manufacturer's interview form, the maximum plasma concentration (C_{max}) and AUC are directly proportional to the dose in Japanese healthy male subjects. After oral administration of 160 mg of valsartan, the C_{max} is 12 μM and the plasma unbound fraction is 5 to 7% (Colussi et al., 1997), indicating that the unbound plasma concentration of valsartan is 0.60 to 0.84 μM. This value is lower than the K_m values obtained from OATP-expressing systems and human hepatocytes. This is consistent with the fact that valsartan exhibits linear pharmacokinetics over the clinical dose range. The absolute value of the uptake clearance of reference compounds in each batch of hepatocytes was different from the reported values (Hirano et al., 2004). We have sometimes experienced that the viability of the hepatocytes and the uptake clearance of compounds are different between the individual tubes even when they are prepared from the same human liver. To overcome this problem, we always check the uptake clearance of reference compounds such as $E_2$17βG in parallel with the test compounds and the relative values of the uptake clearance of reference compounds and test compounds can be discussed.

Regarding the contribution of OATP1B1 and OATP1B3 to the hepatic uptake of valsartan, our results indicate that both OATP1B1 and OATP1B3 are involved in the uptake of valsartan in human hepatocytes, although the estimated contribution of each batch of hepatocytes was different (Table. 3). Previous reports suggest that pitavastatin, a novel 3-hydroxy-3-methylglutaryl CoA reductase inhibitor, and estradiol-17β-glucuronide, a typical substrate of both OATP1B1 and OATP1B3, are taken up into hepatocytes predominantly via OATP1B1 (Hirano et al., 2004), whereas the hepatic uptake of fexofenadine, an H_2-receptor antagonist, is thought to be mainly via OATP1B3 rather than OATP1B1 (Shimizu et al., 2005). Therefore, although OATP1B1 is generally believed to be responsible for the hepatic uptake of several kinds of drugs, we think that the relative importance of OATP1B1 and OATP1B3 depends on the drugs themselves, and this estimation method is useful for predicting their contribution to hepatic clearance. Very recently, we found that telmisartan is recognized exclusively by OATP1B3, and not OATP1B1 (Ishiguro et al., 2006). So, even within the same category of drugs, the relative contribution of OATP1B1 and OATP1B3 is different. This might result in differences in the pharmacokinetics and subsequent pharmacological effects when the function of certain transporters is changed by a variety of conditions, such as genetic polymorphism (e.g., OATP1B1*15) (Nishizato et al., 2003). Therefore, we think that it is important to evaluate the contribution of each transporter to the hepatic elimination of drugs because we can then estimate the change in the overall hepatic clearance quantitatively when the expression level and/or transport function of certain transporters is changed by pathophysiological conditions, single-nucleotide polymorphisms, and

TABLE 5

Summary for the pharmacokinetic parameters of valsartan in SD rats and EHBRs

Pharmacokinetic parameters are expressed as mean ± S.E. (n = 3).

	$AUC_{0-\infty}$	V_1	CL_p	Liver Concentration	CL_{bile}
	μg · min/ml	*ml/kg*	*ml/min/kg*	*ng/g liver*	*ml/min/kg*
SD rat	58.9 ± 9.1	76.3 ± 7.0	17.8 ± 2.5	1.41 ± 0.22	12.5 ± 1.0
EHBR	991 ± 32**	49.0 ± 0.8*	1.01 ± 0.03**	3.45 ± 0.19**	0.283 ± 0.010**

* $P < 0.05$, ** $P < 0.01$.

transporter-mediated drug-drug interactions. This kind of information may make it possible to predict the pharmacokinetics and subsequent pharmacological effects and side effects of drugs under certain conditions.

Next, to identify which transporters are involved in the biliary elimination of valsartan, we investigated the transcellular transport of valsartan in MDCKII cells coexpressing OATP1B1/MDR1, OATP1B1/MRP2, and OATP1B1/BCRP. As a result, the basal-to-apical transcellular transport of valsartan in OATP1B1/MRP2 double transfectant was the largest among three kinds of double transfected cells, whereas that in OATP1B1/MDR1 transfectant was slightly observed, and any significant transport could not be observed in OATP1B1/BCRP transfectant (Fig. 5). In parallel, we observed significant vectorial transport of estradiol-17β-glucuronide in OATP1B1/MDR1, OATP1B1/MRP2, and OATP1B1/BCRP double transfected cells at the same level as in a previous report (Matsushima et al., 2005). The ratio of the basal-to-apical transport to that in the opposite direction in OATP1B1/MRP2 cells was the highest among these double transfectants in the case of estradiol-17β-glucuronide and pravastatin (Matsushima et al., 2005), which were reported to be excreted mainly via MRP2, judged from the impairment of the biliary excretion in EHBR, an Mrp2-deficient rat (Yamazaki et al., 1997; Morikawa et al., 2000). These results suggest that valsartan is also mainly excreted by MRP2. We observed the saturation of transcellular transport in OATP1B1/MRP2 double transfectants with a K_m value of 27.5 μM (Fig. 6a; Table. 4). This K_m value is smaller than that of the efflux transport across the apical membrane (PS_{apical}) (99.0 μM) (Fig. 6b; Table. 4). From a kinetic viewpoint, if the intrinsic efflux clearance across the apical membrane, on which efflux transporters are over-expressed in MDCKII cells, is larger than that across the basal membrane, the transcellular clearance is almost equal to the uptake clearance. Therefore, the K_m value of transcellular transport represents that of OATP1B1-mediated uptake clearance. From our results, the K_m value of transcellular transport was greater than that of uptake by OATP1B1 in HEK293 cells. This discrepancy may be due to the fact that the host cells are different or the uptake process is not a rate-limiting step for the transcellular transport of valsartan. We also checked the ATP-dependent uptake of valsartan in MRP2-expressing membrane vesicles and found time-dependent saturable uptake (Fig. 7). The K_m value obtained from membrane vesicles is smaller than that of PS_{apical} in OATP1B1/MRP2 double transfectants. This is reasonable because we did not estimate the unbound intracellular concentration of valsartan in double transfectants, and the K_m value normalized by the unbound concentration should be lower than the current value.

In addition, we examined the biliary excretion of intravenously administered valsartan in SD rats and EHBRs, in which the MRP2 expression is hereditarily defective. The elimination of valsartan from blood was drastically delayed in EHBRs compared with SD rats, and the biliary excretion clearance in EHBRs was 44 times lower than that in SD rats (Fig. 8), indicating that MRP2 is responsible for the biliary excretion of valsartan, at least in rats. The contribution of transporters might show a species difference. However, taking the results of the transcellular transport in double transfected cells and the ATP-dependent uptake in MRP2-expressing membrane vesicles into consideration, it appears that MRP2 also plays an important role in the biliary excretion in humans.

Further investigations will be required to determine the contribution of efflux transporters to the overall biliary excretion in humans by quantitative comparison of the relative expression levels of each transporter in double transfectants and human liver samples. Information about the contribution of each transporter to hepatic drug transport will be provided by clinical studies investigating the effect of genetic polymorphisms in certain transporters on the pharmacokinetics of different drugs.

In conclusion, we have demonstrated that both OATP1B1 and OATP1B3 are responsible transporters for the hepatic uptake of valsartan, and the efflux clearance of valsartan is mainly via MRP2.

Acknowledgments. We are grateful to Masaru Hirano (The University of Tokyo, Tokyo, Japan) for helpful advice and to Satoshi Kitamura (The University of Tokyo, Tokyo, Japan) for supporting our experiments. We also express our great appreciation to Novartis Pharma AG (Basel, Switzerland) for providing us 3H-labeled and unlabeled valsartan and to Dr. Yuko Tsukamoto and Dr. Ryosei Kawai (Novartis Pharma K.K., Tokyo, Japan) for fruitful discussion.

References

Abe T, Unno M, Onogawa T, Tokui T, Kondo TN, Nakagomi R, Adachi H, Fujiwara K, Okabe M, Suzuki T, et al. (2001) LST-2, a human liver-specific organic anion transporter, determines methotrexate sensitivity in gastrointestinal cancers. *Gastroenterology* **120**:1689–1699.

Chandra P and Brouwer KL (2004) The complexities of hepatic drug transport: current knowledge and emerging concepts. *Pharm Res (NY)* **21**:719–735.

Colussi DM, Parisot C, Rossolino ML, Brunner LA, and Lefevre GY (1997) Protein binding in plasma of valsartan, a new angiotensin II receptor antagonist. *J Clin Pharmacol* **37**:214–221.

Evers R, Kool M, van Deemter L, Janssen H, Calafat J, Oomen LC, Paulusma CC, Oude Elferink RP, Baas F, Schinkel AH, et al. (1998) Drug export activity of the human canalicular multispecific organic anion transporter in polarized kidney MDCK cells expressing cMOAT (MRP2) cDNA. *J Clin Investig* **101**:1310–1319.

Flesch G, Muller P, and Lloyd P (1997) Absolute bioavailability and pharmacokinetics of valsartan, an angiotensin II receptor antagonist, in man. *Eur J Clin Pharmacol* **52**:115–120.

Hagenbuch B and Meier PJ (2004) Organic anion transporting polypeptides of the OATP/SLC21 family: phylogenetic classification as OATP/SLCO superfamily, new nomenclature and molecular/functional properties. *Pflueg Arch Eur J Physiol* **447**:653–665.

Hirano M, Maeda K, Shitara Y, and Sugiyama Y (2004) Contribution of OATP2 (OATP1B1) and OATP8 (OATP1B3) to the hepatic uptake of pitavastatin in humans. *J Pharmacol Exp Ther* **311**:139–146.

Hirano M, Maeda K, Shitara Y, and Sugiyama Y (2006) Drug-drug interaction between pitavastatin and various drugs via OATP1B1. *Drug Metab Dispos* **34**:1229–1236.

Hirouchi M, Suzuki H, Itoda M, Ozawa S, Sawada J, Ieiri I, Ohtsubo K, and Sugiyama Y (2004) Characterization of the cellular localization, expression level and function of SNP variants of MRP2/ABCC2. *Pharm Res (NY)* **21**:742–748.

Hsiang B, Zhu Y, Wang Z, Wu Y, Sasseville V, Yang WP, and Kirchgessner TG (1999) A novel human hepatic organic anion transporting polypeptide (OATP2). Identification of a liver-specific human organic anion transporting polypeptide and identification of rat and human hydroxymethylglutaryl-CoA reductase inhibitor transporters. *J Biol Chem* **274**:37161–37168.

Ishiguro N, Maeda K, Kishimoto W, Saito A, Harada A, Ebner T, Roth W, Igarashi T, and Sugiyama Y (2006) Predominant contribution of OATP1B3 to the hepatic uptake of telmisartan, an angiotensin II receptor antagonist, in humans. *Drug Metab Dispos* **34**: 1109–1115.

Kullak-Ublick GA, Ismair MG, Stieger B, Landmann L, Huber R, Pizzagalli F, Fattinger K, Meier PJ, and Hagenbuch B (2001) Organic anion-transporting polypeptide B (OATP-B) and its functional comparison with three other OATPs of human liver. *Gasteroenterology* **120**: 525–533.